THERMAL CYCLE EFFECTS ON STAINLESS STEEL SENSITIZATION

Cesar A. Cedeño
B.S., Instituto Politecnico Nacional
Mexico D.F.
1981

A thesis submitted to the faculty of the
Oregon Graduate Institute
of
Science and Technology
in partial fulfillment of the
requirements for the degree
Master of Science
in
Materials Science and Engineering

April 1990

This thesis "Thermal Cycle Effects on Stainless Steel Sensitization" has been examined and approved by the following Examination Committee:

David G. Atteridge
Associate Professor
Thesis Research Advisor

Jack H. Devletian
Professor

Rao Gudimetla
Professor

Lawrence E. Murr
Professor and Chairman
Department of Metallurgical
and Materials Engineering
University of Texas El Paso
El Paso, Texas

Stephen M. Bruemmer
Technical Group Leader
Pacific Northwest Laboratory
Richland, Washington

ACKNOWLEDGEMENTS

The author gratefully acknowledges the Division of Engineering Technology, Office of Nuclear Regulatory Research, U.S. Nuclear Regulator Commission for providing financial support of this research and the Latin American Scholarship Program of American Universities for scholarship funding that made this thesis possible.

This work would not have been possible without the patience and understanding of my research advisor, Dave Atteridge. Thanks are also extended to my research committee, Jack Devletian, Rao Gudimetla, Larry Murr, and Steve Bruemmer.

I wish to thank Jessie Atteridge for her assistance in typing, formatting, and editing of this thesis.

CONTENTS

TABLES

FIGURES

THERMAL CYCLE EFFECT ON STAINLESS STEEL SENSITIZATION

Cesar A. Cedeño, M.S.
Oregon Graduate Center, 1988

Supervising Professor: David G. Atteridge

ABSTRACT

Work for this study was directed towards quantifying sensitization development (defined as grain boundary chromium depletion) in high carbon Type 304 and 316 stainless steel (SS) subjected to linear heating to a given peak temperature followed by linear cooling through the sensitization development temperature range. The major variables investigated included: 1. heating rate; 2. peak temperature; 3. holding time at peak temperature; and, 4. cooling rate. Change in sensitization was tracked using the electrochemical potentiokinetic reactivation (EPR) test. Continuous heating/cooling cycles were performed using a furnace or using a thermal cycle simulation machine (Gleeble).

Sensitization was found to increase with increasing peak temperature until a "critical" peak temperature was reached. Sensitization was very low for all samples heated above this critical peak temperature. The critical peak temperature was 900°C for high-carbon (0.06 wt%) 304 and varied from 950 to 1000°C for high-carbon (0.06 wt%) 316 SS. Sensitization increased with decreasing cooling rate and appeared to decrease with increasing heating rate. The slowest heating rate used was equal to the fastest cooling rate tested. Results are discussed in terms of grain boundary chromium carbide nucleation and precipitation, and chromium depletion.

1.0 INTRODUCTION

Sensitization is associated with a loss of corrosion resistance in stainless alloys after heat treatment in, or slow cooling through, an intermediate temperature regime. Corrosion susceptibility results when chromium rich carbides precipitate at grain interfaces causing chromium depletion of adjacent matrix. Development of sensitization is controlled by the thermodynamics of carbide precipitation and kinetics of chromium diffusion, and for the most part has been studied for isothermal heat treatment exposures.

Microstructure development in engineering materials rarely results from simple isothermal heat treatments. Continuous cooling thermal cycles with or without the presence of strain are more common exposures encountered in the real world. Processing, fabrication procedures and service conditions of austenitic stainless steels (SS), for example, reflect this sort of thermomechanical histories. However, limited mechanistic understanding of the effect of thermomechanical history on sensitization has been reported.[1-11]

This study was undertake to develop a basic understanding of sensitization development in austenitic SSs under continuous cooling heat treatments. This is a first step towards understanding and modeling realistic thermomechanical effects on sensitization development. The extent of sensitization in high carbon Type 304 and 316 SS has been studied for various heat treatment cycles by varying parameters

such as peak temperature, cooling rate, heating rate and holding time at peak temperature. Thermal cycles were performed using a furnace or using a microprocessor controlled thermal cycle simulator (Gleeble). Degree of sensitization (DOS) was measured by the electrochemical potentiokinetic reactivation (EPR) test. The results are discussed in the light of carbide nucleation/growth, carbide dissolution, and carbide renucleation/growth occurring during heat treatment cycles.

2.0 BACKGROUND

2.1. SENSITIZATION

Numerous studies[1-14] have been undertaken to understand various aspects of SS sensitization. Although much has been published on sensitization development of austenitic SSs exposed to isothermal heat treatment, very little published information is focused on the effects of continuous cooling heat treatments on sensitization. A review of the major factors effecting sensitization development is presented below.

It is hypothesized that DOS is controlled by grain boundary chromium depletion. This theory was first suggested by Bain, et al[12] and was quantized by Strawstrom and Hillert,[13] and Tedmon et al.[14] It is the most accepted theory used to explain the loss of corrosion resistance in austenitic SS. The chromium depletion model attributes sensitization to the development of a chromium depleted zone adjacent to the grain boundaries due to precipitation of chromium rich carbides. Bain, et al[12] suggested that chromium rich carbides will precipitate at grain boundaries if given sufficient time in the temperature region where carbides are stable. The diffusivity of carbon, which diffuses as an interstitial, is much higher than that of chromium, which must diffuse substitutionally. The differences in diffusivities give rise to a chromium depleted zone adjacent to the grain boundaries during carbide growth.

2.2. PARAMETERS AFFECTING SENSITIZATION

Sensitization development in austenitic SSs is controlled by alloying elements (in particular carbon and chromium) and other variables such as dislocation density that affect the thermodynamics and/or kinetics of carbide precipitation.

2.2.1. Carbide Precipitation

Sensitization of austenitic SS requires the precipitation of chromium-rich carbides along grain boundaries. In the absence of any strong carbide forming element, $M_{23}C_6$ is the carbide formed. Carbide precipitation at grain boundaries has been widely studied. These studies have documented carbide morphology,[15-20] composition and crystal structure.[16] $M_{23}C_6$ is mainly composed of chromium carbide, so the designation $Cr_{23}C_6$ is frequently used. However, since other elements can partially substitute for chromium, other nomenclatures have been reported, i.e., $(Cr,Fe)_{23}C_6$, in 304 SS or $(Cr,Fe,Mo)_{23}C_6$ in 316 SS.[15]

Many investigations have been carried out concerning the precipitation behavior of $M_{23}C_6$ under isothermal heat treatment. Figure 1 shows a typical temperature-time-carbide precipitation (initiation) curve for a high carbon Type 316 austenitic SS.[21] On the other hand, few investigations dealing with precipitation during complex thermal cycles have been conducted.[22]

Austenitic SSs are conventionally subjected to a high temperature solution treatment followed by a severe quench. It is hypothesized that carbide

embryos/precipitates formed during the prior quench and/or heating portion of a thermal treatment promote rapid sensitization development when specimens are isothermally held in, or slow cooled through the sensitizing temperature range. The rate of sensitization appears to decrease substantially if the SS is again heated to temperatures near the solution treatment temperatures and then slow cooled through the sensitization development regime.

Ikawa, et al,[22] have studied the precipitation phenomena of $M_{23}C_6$ during thermal cycles. They adopted two different heat treatments; one consisted of heating specimens directly to selected isothermal holding temperatures after an initial solution heat treatment followed by a rapid quench while the other consisted of initially heating specimens to 1100°C, holding for 2 minutes, and then rapidly cooling to selected isothermal holding temperatures (Figure 2). The C-curve representing time for initial carbide precipitation for specimens heated directly to isothermal hold temperatures (Curve 1) developed grain boundary carbides at shorter times than the specimen set subject to 1100°C prior to reaching isothermal hold temperatures (Curve 2). It was concluded that this shift in precipitation time was due to dissolution at 1100°C of prior grain boundary embryos/precipitates. This necessitated increased precipitate nucleation times during the subsequent isothermal hold portion of the heat treatment.

A diagram of carbon solubility for different carbon composition in Type 304 and 316 austenitic stainless steels is shown in Figure 3. The curves were calculated using the carbon solubility equations reported for Type 304 and 316 by Natesan and

Kassner[23] and Deighton.[24] It is assumed complete embryo/precipitate dissolution takes place at temperatures above the two phase field.

2.2.2. Influence of Composition

It is important to recognize that many of the austenitic alloys, and in particularly the stainless steels, are in a nonequilibrium, metastable state at use temperatures. Thus the extent kinetic processes approach the thermodynamic equilibrium state during heat treating is a major factor in determining subsequent corrosion behavior of the alloy.

Sensitization behavior can also be controlled by varying the alloy chemistry. An increase in corrosion resistance is (generally) accomplished by removing carbon and/or adding "stabilizing" elements such as Nb or Ti, which are stronger carbides former than chromium.[25] They tie up the carbon, thus reducing the amount of intergranular chromium carbide. This minimizes the formation of the chromium-depleted zone adjacent to the grain boundaries.

2.2.2.1. Carbon The carbon content of austenitic SS is the most significant compositional factor determining the ultimate susceptibility of the alloy to sensitization development. The more carbon present the faster the rate of sensitization development and the greater the sensitization development temperature regime. This is illustrated by the time-temperature-sensitization (TTS) curves for

several carbon concentrations seen in Figure 4.[1,3] The curves represent the conditions necessary to develop a given DOS level as a function of carbon concentration and temperature.

2.2.2.2. Major Substitutional Alloying Element The major substitutional alloying elements in SS (such as chromium, nickel, molybdenum) can significantly effect the susceptibility of austenitic SS to intergranular corrosion. For example, chromium has a pronounced effect on the passivation of SSs, so it is not surprising that there is a relationship between the DOS and chromium concentration. It has been found that variations in the susceptibility to intergranular attack are determined primarily by changes in chromium content.[12] Those regions of the steel where the local chromium composition falls below about 12% have a diminished ability to form a passive film. It is generally believed that the resistance of sensitization increases with increased chromium content. Chromium is a strong compound-former; in particular, it readily forms carbides and nitrates if carbon and nitrogen are present in sufficient concentrations.

Likewise, molybdenum appears to contribute to the ease with which steels passivate. Also, this element tends to raise the temperature[26] at which carbides will form on heating in stainless steel. The effect of molybdenum on austenitic stainless steel is, in general, to decrease rate of susceptibility development. In contrast, nickel does not affect sensitization behavior but is required in order to stabilize the

austenite phase field. The nickel content of austenitic stainless steels generally increased as the chromium concentration of the alloy increases.

In addition, the presence of cold work prior to and/or strain during thermal cycling has been shown to enhance sensitization development.[1,2,9,11,27]

2.3. CONTINUOUS COOLING SENSITIZATION

Microstructure development in engineering materials rarely results from simple isothermal heat treatments. Processing and fabrication procedures entail combinations of thermal and thermomechanical exposures. Continuous cooling, where the maximum temperature and subsequent cooling rate control microstructure development, represents a common thermal exposure.

Time-temperature-sensitization curves represent conditions necessary for the isothermal development of a sensitized microstructure. However, they can also be used to indicate continuous cooling sensitization development even though they can not be used directly to determine the extent of sensitization development that occurs when materials are exposed to continuous cooling thermal cycles. This is because they do not take into account the effect of time spent at different temperatures, the maximum temperature the specimen reaches prior to low temperature exposure, or the thermomechanical history a material may be subjected to.

Attempts to predict a critical cooling rate for sensitization during continuous cooling have been made.[5,28] One approach that has been adopted is the Mannig-

Loring method[29] which is used to obtain low carbon steel alloy continuous cooling transformation curves from isothermal time-temperature curves.

In this method, a cooling curve is simulated by a series of small continuous cooling segments, where ΔT is the temperature difference in each segment. The time of transit (Δt) is determined for each segment of the cooling curve and is divided by the isothermally determined sensitization time (t_s) for the mean temperature of each segment (Figure 5). It is then assumed that sensitization occurs when the summation of these partial contributions, as defined by Equation 1, is unity.[28]

$$\alpha = \sum_{T_H}^{T_L} \frac{\Delta t}{(t_S)_T} \qquad (1)$$

The major drawback of this approach is that the model predicts that sensitization development, at a constant cooling rate, is independent of peak temperature above the maximum sensitization development temperature predicted by the TTS curve. Experimental evidence has conclusively shown that this is not so.[1,2,8,11] Ikawa, et al,[22] overcame this drawback by assuming that the TTS curve characteristics changed as a function of peek temperature (Figure 1).

Bruemmer has developed a PC-Basic sensitization development model which predicts DOS as a function of thermomechanical treatment versus simply predicting sensitization initiation as in the Ikawa et al approach.[1,2] Bruemmer's model is based on a large isothermal experimental data base and predicts continuous cooling sensitization by addition of normalized isothermal sensitization time steps.

The Bruemmer model is theoretically based but empirically modified to fit a limited continuous cooling data base.[1] Further development of continuous cooling sensitization understanding and modeling capability requires development of a substantial continuous cooling data base. The work reported herein initiates the development of such a data base.

3.0 EXPERIMENTAL PROCEDURE

3.1. MATERIALS

Commercially available heats of Type 304 and 316 SS were obtained to evaluate the effect of continuous cooling heat treatments on the development of sensitization. Materials were received from Battelle Pacific Northwest Laboratory (PNL) as part of an ongoing study originally initiated at PNL and now jointly continued at PNL and the Oregon Graduate Center. The material was studied in the mill annealed condition. Chemical composition of the various heats under study are given in Table 1.

3.2. THERMAL CYCLE SIMULATION

Thermal cycles for simulating various continuous cooling heat treatments were carried out using two techniques. Initial experimentation was carried out using an Electric Muffle Furnace, Model 7022-A-3. Further evaluation was carried out using a thermal processing simulator, Duffers Gleeble.

3.2.1. Thermal Cycling Using an Electric Muffle Furnace

As-received, mill-processed austenitic SS 10 cm diameter pipes were sliced into 1.25 cm-thick rings. Sections 1.25 X 1.25 cm were subsequently cut off these

rings (Figure 6). Cutting was carried out using a vertical band saw flooded with coolant so as to avoid any excess heating that might alter the properties of the specimens.

Two samples from each heat were taken for each test. To ensure a homogeneous temperature, the samples were tightly packed in a SS box. Sample temperature was recorded from two chromel-alumel thermocouples which were spot welded on two different samples. A typical continuous cooling temperature versus time curve is shown in Figure 7.

Furnace treatments were used to determine the effect of peak temperature and cooling rate on the development of sensitization in the four SS heats given in Table 1. Experiments included studying the effects of maximum temperature (800, 850, 900, 950, 1000, 1050, and 1100°C) and four cooling rates (0.05 to 2°C/sec) from each maximum temperature on sensitization. Actual "effective" cooling rates that were achieved for specimens heated to peak temperatures between 800 and 1100°C in the furnace are shown in Table 2. The cooling rate reported is the average cooling rate between 800 and 600°C.

A variety of procedures were used to achieve different cooling rates on different samples. Higher cooling rates of 1.5 to 2°C/sec (cooling rate 1) were obtained by removing specimens from the furnace and cooling in open air. A cooling rate of 0.7 to 1°C/sec (cooling rate 2) was accomplished by placing specimens inside an austenitic SS pipe, heating to the required peak temperature and

then air cooling. Cooling rates of 0.10°C/sec (cooling rate 3) and 0.05°C/sec (cooling rate 4) were achieved by keeping the specimens inside the furnace with furnace door open and closed, respectively.

It should be noted that cooling was immediately commenced once the peak temperature had been reached for the higher cooling rates (cooling rates 1 and 2). However, there was approximately a 20 second delay at the peak temperatures before specimen cooling started for the slower cooling rates (cooling rate 3 and 4).

3.2.2. Simulation of Thermal Cycles Using a Thermal Processing Simulator (Gleeble)

Studies on continuous cooling sensitization development on various heats of high carbon Type 304 and 316 of SS (Table 1) were carried out using a furnace (outlined above). Additional work was carried out on one Type 316 SS. Heat (SS16) in a more systematic way by using a microprocessor controlled thermal processing simulator (Gleeble) in order to establish a basic understanding of the sensitization development in austenitic SS during continuous cooling.

Specimens 15.2 cm in length and 1.3 cm in width were placed between two SS wedge jaws on the Gleeble. The jaws were designed so as to provide a good electrical contact with the specimen. A uniform work zone of length 1.3 cm was obtained during simulated thermal cycles irrespective of the maximum temperature. This work zone had a negligible thermal gradient (Figure 8), and material was taken from this zone for subsequent sensitization studies (see Section 3.3).

The desired continuous cooling cycles were achieved within the work zone by pre-programming required thermal cycle parameters (heating rate, peak temperature, holding time, cooling rate, and minimum temperature) into the control computer. A typical time-temperature plot (Figure 9) illustrates the linearity in the heating and cooling rates that were obtained during a simulated thermal cycle. This was much better control than found in the thermal cycles obtained using the furnace.

Tests were performed in the maximum temperature range of 950 to 1050°C. This range of temperature was chosen because it was the critical transition temperature where EPR-DOS was found to change from high to low values for the furnace treated specimens. A schematic representation of the experimental thermal cycles is shown in Figure 10 as a function of peak temperature. The matrix of experimental thermal cycles is shown in Table 3.

3.3. SENSITIZATION MEASUREMENT

A number of chemical and electrochemical corrosion tests have been used to assess sensitization in austenitic SSs. Five of these have been qualified for many years as ASTM Standard Test Procedures (A272-77a).[30] The difficulties with these test are that they are destructive and qualitative in nature. To overcome these limitations, a rapid, quantitative and nondestructive method called the EPR test has been used in this study to estimate the DOS of the various specimens.

3.3.1. Sample Preparation for EPR-Test

Heat-treated specimens were attached to a SS screw and mounted in an acrylic plastic. Specimens were subsequently metallographically wet ground to 600 grit using silicon carbide abrasive paper and diamond polished to 1 μm level. The samples were then masked using a specimen area tape. The area tape provides a convenient method to define the area of the specimen used for testing. Electrochemical potentiokinetic reactivation-DOS values were obtained using a fresh solution of 0.5M H_2 SO_4 + 0.01 M KSCN at 30°C. The EPR test conditions used are summarized in Table 4.

3.3.2. EPR-Test Procedure

Electrochemical potentiokinetic reactivation tests were performed using an InstruSpec Model WC-5 Metal Sensitization Detector specifically designed for automated single-scan EPR testing. The EPR test procedure consists of initially determining corrosion potential. The specimen is then taken to the passivation potential and held for 2 minutes to assure development of a passive oxide film on the surface of the sample. This oxide film tends to protect the underlying matrix from corrosion during subsequent reactivation.[31] The potential is then swept in reverse from the passive through the active region (reactivation) down to the corrosion potential in the electrolyte mentioned above. The break down of the passivated film is a function of chromium depletion. Figure 11 shows a

representation of typical potentiokinetic reactivation curves for a nonsensitized and sensitized material during EPR-test.

Quantitative measurement of DOS is based on relationships introduced by Clarke, et al.[31] According to Clarke, DOS can be related to the integrated area under the reactivation curve (charge Q in Coulombs) resulting from corrosion of the chromium depleted zone, normalized to the area of the sample exposed and the total grain boundary area (GBA) tested, to give the charge per square centimeter of grain boundary, Pa or EPR-DOS. This relationship is given in Equation 2 below:

$$Pa = Q/GBA \qquad (2)$$

where,

Q = reactivation charge (coulomb)

GBA = As ($5.09544X10^{-3}$ EXP 0.34694X) (cm^2)

As = Specimen area (cm^2)

X = ASTM grain size at 100X

It should be noted that Clarke assumed that all attack is confined to the grain boundaries, is uniformly distributed over all grain boundaries, and that the width of boundary attack is constant at 10^{-4} cm.

Calculations of EPR-DOS required determination of the grain size of the specimens. Average grain size measurements were made using the three circles, or Abrams, intercept procedure (ASTM E112-85).[32]

4.0 EXPERIMENTAL RESULTS

4.1 CONTINUOUS COOLING INDUCED SENSITIZATION DEVELOPMENT

Sensitization development resulting from continuous cooling has been studied for various heat treatment cycles in both Type 304 and 316 SS. A number of parameters were examined using two thermal Simulation techniques. The first set of experiments were performed using an Electric Muffle furnace. The second required usage of a microprocessor controlled thermal cycle simulator (Gleeble).

The results obtained from the different continuous cooling methods are presented separately in the following sections. Reported EPR-DOS values are obtained by normalizing the charge during reactivation with the specimen area and the grain size. The average grain size of all alloys was determined to be approximately 60 μm (5.2 ASTM at 100X).

4.1.1. Continuous Cooling Sensitization Development in Furnace Treated Specimens

The effect of continuous cooling heat treatment on sensitization was examined on four heats of high carbon austenitic SS (Table 1). Peak temperatures achieved during each heat treatment cycle were varied from 800 to 1100°C. Cooling rates following achievement of peak temperature ranged from 0.05 to 2°C/s. The focus of the experimental work was to determine the influence of peak temperature and

cooling rate on sensitization development. The results experimentation are presented in tabular form in Tables 5 through 8, and are discussed below.

The cooling rate reported for the electron muffle furnace specimens is the average cooling rate between 800 and 600°C. This cooling rate is greater than the actual cooling rate of temperatures above 800°C and less than the cooling rate below 600°C (see Figure 7). It is close to the measured cooling rate between 800 and 600°C but actually only correct around a temperature of 700°C.

It is felt that the use of this estimated cooling rate is appropriate as the majority of sensitization is expected to take place in the 800 to 600°C range with little or no increase in sensitization development below 600°C.

4.1.1.1. Peak Temperature Effect on Sensitization The parameter of peak temperature appears to be a critical factor in the development of sensitization in the different heats studied. The DOS (as measured by EPR) increases as a function of peak temperature in the temperature range between 800 and 900°C in the Type 304 heats. A further temperature increment results in a decrease in the EPR-DOS value. Thus 900°C appears to be a critical peak temperature for Type 304 sensitization development. This behavior is observed at all cooling rates examined [Figures 12 (a) and (b)]. This drop in DOS versus peak temperature beyond a certain critical peak temperature has been observed by other investigators.[1,3]

A similar pattern of behavior appears to be present in the Type 316 heats [Figures 13 (a) and (b)]. The only differences is that the critical peak temperature for the decrease in DOS seems to be dependent on cooling rate and, in general, is higher than for Type 304 SS.

The critical peak temperature for Type 316 Heat SS16 appears to shift to higher values (between 950-1000°C) as the cooling rate increases. The only exception is that the specimen experiencing a cooling rate of 0.10°C/s has a critical temperature between 900 to 950°C. Likewise, heat Type 316 SS17 has a critical peak temperature between 950 and 1000°C at higher cooling rates (0.92 to 2°C/s), and 900 to 950°C at slower cooling rates (0.05 to 0.10°C/s).

4.1.1.2. Cooling Rate Effect on Sensitization Cooling rate effects on sensitization development have been examined for different peak temperatures. The general trend observed is that the DOS increases with decreasing cooling rate.

At a fixed peak temperature, Type 304 heats (SS6 and SS7) exhibit comparably low EPR-DOS values for higher cooling rates (0.92 to 2°C/s) and comparably higher EPR-DOS for the lower cooling rates (0.11 to 0.05°C/s) with EPR-DOS increasing with decreasing cooling rate. This increase in EPR-DOS values is found to be higher for heat SS6 than SS7 [Figures 14 (a) and (b), and Figures 15 (a) and (b), respectively].

Type 316 heats [SS16 and SS17, Figures 16 (a) and (b), and Figures 17 (a) and (b), respectively] show similar DOS behavior as a function of cooling rate as

seen in the Type 304 heats. Samples experiencing slower cooling rates develop higher DOS than specimens heat treated at higher cooling rates for a given peak temperature. Both Type 304 and 316 material remain unsensitized when heated to peak temperature above 1050°C and cooled at rates faster than 0.9°C/s. A major difference between Type 304 and 316 is that Type 304 appears to sensitize to a greater extent at temperatures greater than peak temperature and cooling rates slower than 0.1°C/sec (see Figure 12 versus 13). This effect is not completely understood but is attributed to the effect of the increased molybdenum in the Type 316 alloys.

Specimens of Type 316 SS16 heat treated at cooling rates varying from 1.12 to 2°C/s for peak temperatures in the range of 1050 to 1100°C, as well as those heat treated at cooling rates varying from 1.46 to 1.67°C/s in the temperature range of 800 to 850°C, are unsensitized. Type 316 Heat SS17 specimens show a similar tendency of non-sensitized microstructure, with the only exception being the sample heat treated at 850°C and slow cooled at 1.76°C/s.

4.1.2 Continuous Cooling Sensitization Development in Gleeble Treated Specimens

A microprocessor controlled thermal processing simulator was used to study the effect of peak temperature, cooling rate, heating rate and holding time on sensitization development. The Gleeble, as outlined earlier, provides excellent control of the heat treatment cycles; thus, more controlled experiments are possible using this technique than the furnace technique.

Initial Gleeble experiments consisted of "duplicating" the furnace thermal cycles for the slowest cooling rate used in the furnace experimentation. Critical studies to determine the effect of heating rate and holding time on sensitization development during heat treatment cycles were then examined. The Type 316 Heat SS16 was selected for use in this Gleeble study. Data obtained is presented in tabular in Tables 9 and 10, and discussed below.

4.1.2.1 Peak Temperature Effect on Sensitization Initial test results obtained in the peak temperature range of 800 to 1100°C show an increase in EPR-DOS values as peak temperature increases from 800°C up to 1000°C. Degree of sensitization then decreases as temperature is further increased (Figure 18). These values were consistent with the set of test results obtained during previous furnace experimentation with the exception that the critical peak temperature found in the Gleeble study was 1000°C versus 950°C for the furnace study (Figure 18).

Further tests were performed in the peak temperature regime of 950 to 1050°C near the critical peak temperature to study the effect of peak temperature on DOS development. Peak temperatures of 975, 1015, and 1025°C were studied to better map the critical region (EPR-DOS obtained are tabulated in Table 10). These studies show that the DOS value increases up to 1000°C and that a further temperature increment of 15°C results in a drastic decrease in EPR-DOS values (Figure 18).

4.1.2.2. Cooling Rate Effect on Sensitization Development of sensitization for the SS16 heat as a function of cooling rate was examined by varying cooling rates from 0.05 to 2°C/s. Results obtained are shown in Figure 19. The figure shows that EPR-DOS values increase as cooling rate decreases. It can also be observed that sensitization development depends not only on cooling rate but also on the peak temperature achieved during heat treatment cycle.

4.1.2.3. Heating Rate Effect on Sensitization In order to determine the effect of heating rate on sensitization development in austenitic stainless steels during continuous cooling heat treatment cycles, critical experiments were performed using the two heating rates of 2 and 50°C/s. Effect of heating rate was examined as a function of peak temperature, cooling rate and holding time.

Electrochemical potentiokinetic reactivation DOS appears to decrease with increasing heating rate regardless of peak temperature (Table 9). This observation is opposite findings reported in previous work by Solomon.[8] Solomon determined that varying the heating rate in the range of 20 to 135°C/s did not effect the extent of sensitization development during heat treatment cycles. But, as the minimum heating rate of 2°C/s used in this study was considerably slower than the minimum rate investigated by Solomon, this result is not necessarily unexpected.

4.1.2.4. Holding Time Effect on Sensitization Several test were conducted to estimate the influence of holding time at peak temperature on sensitization development during continuous cooling heat treatment. Tests were performed by

holding specimens from 0 or 15 minutes in the peak temperature regime of 950 to 1050°C and then subsequently subjecting them to cooling rates of 2 or 0.05°C/s. An additional test was performed by increasing holding time to 30 minutes at 1000°C followed by cooling at 0.05°C/s.

Experimental results show that the DOS increases as holding time increases from 0 to 15 minutes at 950°C at the slower cooling rate. A slight decrease in EPR-DOS value is observed when a specimen is held for 15 minutes at 1000°C; the EPR-DOS value dropped rapidly when holding time at 1000°C was increased from 15 to 30 minutes (Figure 20).

An increase in EPR-DOS is observed at 1050°C as holding time increases from 0 to 15 minutes at the high heating rate (50°C/s) while a decrease in DOS is observed for the slower heating rate (2°C/s).

5.0 DISCUSSION OF RESULTS

5.1 SENSITIZATION DEVELOPMENT DURING CONTINUOUS COOLING CYCLES

The extent of sensitization development during continuous cooling heat treatment cycles is dependent upon such variables as maximum temperature and cooling rate. Likewise, parameters such as heating rate and holding time at maximum temperature appear to influence the tendency for sensitization development in austenitic SSs. Discussion of the possible causes for the observed sensitization development behavior is based on the influence of these variables on carbide nucleation and growth kinetics since this controls sensitization development. Carbide nucleation and growth and, under certain conditions, carbide dissolution during heating will be discussed. Differences between furnace and Gleeble results are discussed where required.

5.1.1 Peak Temperature Effect Austenitic SSs heated to a peak temperature in the range of 800 and 1100°C and then cooled to ambient showed a general trend of increasing DOS with increasing maximum temperature until reaching a certain critical maximum temperature when a precipitous decrease in ambient DOS occurred.

Experimental results for both Type 304 and 316 SS alloys show similar behavior; the only exception is that the critical maximum temperature is higher for the Type 316 heats, see Figures 12 and 13.

5.1.1.1 Type 304 Stainless Steel Heats The increase in DOS when peak temperature is increased from 800 to 900°C, can be qualitatively explained through the use of a TTS plot (Figure 4). The TTS plots depicted in Figure 4 estimate the time required to develop detectable sensitization in austenitic SSs during isothermal holding but can also be used as an indicator of sensitization development during continuous cooling.

The TTS curves illustrate that sensitization is dependent on the thermodynamic of carbide precipitation and kinetics of chromium diffusion. Thermodynamics limit carbide precipitation and sensitization development at high temperatures and also after long times at moderate temperatures. Chromium diffusion limits sensitization development at low temperatures and after short times at moderate temperatures. The combination of these two effects define the "C-curve" which is typical of TTS plots.

Time-temperature-sensitization plots can be used to indicate sensitization development during cooling through the sensitizing temperature range (Figure 21). The extent to which the cooling curve intersects the TTS diagram is an indicator of the time spent in the sensitization range. A first order approximation of the DOS development during a continuous cooling cycle can be based on the amount of time

spent in the sensitization development temperature range. The longer the time in this temperature range, the higher the expected DOS. Thus, one can say that the increases of EPR-DOS observed as the maximum temperature is increased is because cooling time in the sensitization development region increase with increasing maximum temperature. This is illustrated schematically in Figure 21.

This first approximation approach to the prediction of sensitization indicates that DOS should increase with increasing maximum temperature until a critical maximum temperature is reached where an additional increase in maximum temperature would not result in increased time during cooling in the sensitization region. Thus this simple model indicates that sensitization (at a constant cooling rate) should increase with increasing peak temperature until a critical peak temperature is reached and then would be expected to remain essentially constant as peak temperature is raised. However, the experimental results found from continuous cooling experiments demonstrate that this is not so and that, in fact, DOS dramatically drops off with increasing maximum temperature. It is therefore apparent that sensitization development is not simply controlled by the time spent cooling through the sensitization range irregardless of prior thermal history.

It is proposed that insight into the reasons for the dramatic change in DOS with increase peak temperature can be obtained by taking account of carbide solubility characteristics. Calculations from Natesan and Kassner carbon solubility equations[23] for austenitic Type 304 SS indicate that the carbon solubility

temperature for Heats SS6 and SS7 are 941C and 953C, respectively. These temperatures are reasonably close to the measured critical peak temperatures and indicate that continuous cooling sensitization development is dependent upon whether the peak temperature is above or below the carbon solubility temperature. Thus it is proposed that the observed drop in EPR-DOS value at high maximum temperature may be explained based on grain boundary embryo/carbide dissolution on heating above the critical peak temperature and the need for subsequent carbide renucleation during continuous cooling.

This hypothesis is based on the assumption that the original solution heat treatment rapid quench and/or rapid specimen heating prior to initiation of the cooling cycle induces high energy grain boundary nucleation sites, embryos and/or carbides. Therefore, it is assumed that carbide dissolution (and/or a change in localized grain boundary condition) during high temperature exposure will require renucleation of carbides during continuous cooling and effectively shift the TTS curve to longer times (Figure 22).

It is proposed that carbide nucleation and growth can take place with minimal or no need for a nucleation incubation period for peak temperature cycles at and below the critical peak temperature. However, once the critical peak temperature is exceeded all high energy nucleation sites and/or embryos and/or precipitates are dissolved.

Critical nuclei formation is difficult on continuous cooling as the driving force for nucleation is low at high temperatures and the critical nucleation size is large. By the time they are formed the temperature reached is low enough so that only limited, if any, growth takes place. This scenario would explain the experimentally observed results.

5.1.1.2 Type 316 Stainless Steel Heats The Type 316 specimens heat treated in the furnace showed a similar trend to that found in Type 304, that of increasing DOS as maximum temperature increased up to a certain critical peak temperature. The major differences found were that Type 316 reached higher maximum DOS values, that Type 316 had a higher critical peak temperature than Type 304, and Type 304 had higher EPR-DOS values for peak temperatures above critical peak temperature (Figures 12 and 13).

The differences between the sensitization behavior of the alloy types is due to the presence of molybdenum in Type 316, as both have similar carbon concentrations. Increasing molybdenum has been found to shift the TTS curve to longer times and higher temperatures (Figure 23). The presence of molybdenum decreases chromium diffusivity and raises the activity of chromium in the matrix and in equilibrium with the carbide at the interface.[33] This results in sensitization development at higher temperatures in 316 SS than for 304 SS, but the kinetics of sensitization are reduced at comparable temperatures. Molybdenum is also found to

stabilize carbides and therefore molybdenum tends to increase the dissolution temperature of the carbide,[37] and hence the maximum temperature at which DOS can be expected.

5.1.1.3 Comparison of Peak Temperature Effects Using Furnace and Thermal Cycle Simulation Techniques A comparison between furnace-induced and Gleeble-induced sensitization development results for Type 316 Heat SS16 under nominally similar heating and cooling results show identical trends (Figure 18). However, the specimens heat treated in the Gleeble developed lower DOS values at peak temperatures below 1000°C. In addition, the Gleeble-induced maximum critical-peak temperature was higher than that induced in the furnace heated specimens.

Some discrepancies between furnace and Gleeble specimens are to be expected. The cooling rate calculated for furnace specimens is only approximately accurate for a limited (600 to 800°C) cooling range (Figure 7) whereas the Gleeble cooling rate is accurate over the complete cooling cycle (Figure 9). It is entirely possible that the considerably slower cooling rate below 600°C for the furnace cooled specimens resulted in increased DOS development. In addition, the maximum temperature reached during a given cycle and the time near/at maximum temperature was more closely controlled in Gleeble testing.

The experimental data plots also tend to exaggerate the (potential) differences between critical maximum temperature. Gleeble studies indicate less than a 15°C

differences in peak temperature is required to correctly define the critical peak temperature. The furnace cycle peak temperature data indicates that the critical peak temperature lies between 950 and 1000°C while the Gleeble data indicates it lies between 1000 and 1015°C. It is felt this is reasonable agreement between these two differing techniques.

5.1.2 Cooling Rate Effect Similar patterns of behavior are observed for Types 304 and 316 SS as a function of cooling rate at a specific peak temperature with EPR-DOS values increasing as cooling rate decreases. These observations can also be qualitatively deduced by consideration of the intersection of the cooling curve with the sensitization range in a TTS diagram. Slower cooling rates from a given peak temperature will result in a longer residence time in the sensitization regime (Figure 24); hence DOS increases.

The EPR-DOS values are observed to be numerically lower for the Type 316 stainless steels as compared to Type 304 SSs (for the same heat treatment conditions). This is because the time necessary to achieve a given DOS (for a given isothermal heat treatment) increases with increasing molybdenum content,[33] at least within the Type 316 SS molybdenum addition range.

5.1.3 Heating Rate Experimental results tabulated in Table 9, show a small but consistent difference in sensitization development between specimens heat treated at a heating rate of 2 versus 50°C/s. Comparison of EPR-DOS obtained with the two different heating rates (Figure 25) show that sensitization for specimens heated

at slower rate develop higher EPR-DOS. If there was no effect of heating rate, all the data on Figure 25 would be expected to lie on the bisecting straight line or randomly on either side. In contrast, Solomon found that heating rates between 20 and 120°C/s did not effect resultant sensitization, as might be expected due to the high heating rates studied.[8]

This work certainly does not contain a comprehensive study of heating rate effects. It does indicate, however, that a systematic study of variable heating rates might show a large effect on sensitization development with the possibility of a critical heating rate resulting in maximum carbide precipitation and subsequent sensitization.

5.1.4 Holding Time Effect This parameter appears to contribute to sensitization development when peak temperatures are somewhat below the critical peak temperature and contribute to critical peak lowering at temperature near critical peak temperature.

An increase in holding time at a peak temperature of 950°C from 0 to 15 sec increased resultant DOS-EPR from approximately 70 to 80 c/cm^2 while an increase in holding time of 0 to 30 minutes at 1000°C decreased the resultant DOS-EPR from 60 to 8 c/cm^2 see Figure 20. These results indicate that critical peak temperature is a function of time at peak temperature.

6.0 CONCLUSIONS

A continuous cooling sensitization study has been carried out on two high-carbon 304 and two high carbon 316 grade SSs. Thermal cycle simulations for heat treatment were obtained by using two techniques. Initial experimentation was carried out using an Electric Muffle Furnace. Further evaluation of one of the Type 316 SS heats was carried out in a more systematic manner by using a microprocessor controlled thermal processing simulator Gleeble.

Based on the experimental results, the following conclusions were drawn:

1. Among the various parameters studied, the peak temperature and subsequent cooling rate appear to have the most significant influence on the DOS developed during continuous cooling.
2. It has been observed that, irrespective of the peak temperature achieved, DOS increases as continuous cooling rate decreases.
3. The DOS increases as peak temperature increases up to certain critical maximum temperature. Above this critical peak temperature, sensitization development was dramatically reduced during continuous cooling.

4. The results indicate that sensitization development during continuous cooling does not solely depend on the maximum temperature achieved and the cooling rate. It also depends on the heating rate and the holding time at the peak temperature.
5. Although limited experimental data does not allow a firm conclusion, the general trend suggests an increase in DOS with decreasing heating rate.
6. Holding time appears to enhance sensitization during continuous cooling when specimens are held below a critical temperature, assumed to be at or near the carbon solubility (C_s) temperature. Above this critical temperature the DOS decreases with increased holding time.
7. While the mechanisms of sensitization is not completely understood for all situations of interest, especially those above the maximum critical peak temperature, experimental data can be generally understood based on the precipitation and dissolution characteristics.
8. The results of this work indicate that significant progress towards understanding the role of carbide precipitation and/or dissolution on non-

isothermal heat treatment sensitization development could be achieved by determining critical peak temperature as a function of heating rate, holding time and cooling rate. The experiments would need to be carried out in conjunction with step quenching experiments subjected to detailed analysis of carbide nucleation and growth kinetics and thermodynamics.

7.0 TABLES

TABLE 1. Bulk Compositions of Austenitic Stainless Steel, wt%

Label	Type	C	Cr	Ni	Mo	Mn	Si	P	S	N	B
SS6	304	0.058	18.67	8.78	0.16	1.89	0.38	0.012	0.002	0.059	0.001
SS7	304	0.064	19.17	9.54	0.12	1.31	0.42	0.013	0.015	0.041	0.001
SS16	316	0.058	17.11	11.43	2.16	1.77	0.41	0.014	0.005	0.008	0.002
SS17	316	0.070	16.81	11.21	2.20	1.46	0.28	0.016	0.020	0.071	0.003

TABLE 2. Continuous Cooling Rates Obtained in the Furnace

Cooling Rate Number	Peak Temperature, °C						
	800	850	900	950	1000	1050	1100
1	1.46	1.76	1.67	1.58	1.79	1.86	1.99
2	0.71	0.81	0.83	0.88	0.97	1.12	1.14
3	0.08	0.10	0.09	0.10	0.09	0.09	0.10
4	0.05	0.06	0.05	0.06	0.05	0.06	0.06

TABLE 3. Gleeble Experimental Matrix

Temperature °C	Heating Rate °C/s	Holding Time min	Cooling Rate °C/s
950	2	0	2
	50	0	2
1000	2	0	2
	50	0	2
1050	2	0	2
	50	0	2
950	2	0	0.05
	50	0	0.05
1000	2	0	0.05
	50	0	0.05
1050	2	0	0.05
	50	0	0.05
950	2	15	2
	50	15	2
1000	2	15	2
	50	15	2
1050	2	15	2
	50	15	2
950	2	15	0.05
	50	15	0.05
1000	2	15	0.05
	50	15	0.05
1050	2	15	0.05

TABLE 4. Experimental Conditions of EPR Test

Instrument:	InstruSpec Model WC-5 Metal Sensitization Detector
Electrolyte:	0.5 M H_2SO_4 + 0.01 KSCN
Temperature:	30°C
Specimen finish:	1 μm (diamond paste)
Passivation Conditions:	Potential of 0.2V (SCE) for 2 min
Reactivation Scan Rate:	6V/h (AISI 304 SS) 3V/h (AISI 316 SS)

TABLE 5. Peak Temperature and Cooling Rate Effect on Furnace-Induced Sensitization for Type 304 SS Heat SS6

Peak Temperature, °C	Degree of Sensitization, C/cm²			
	1	2	3	4
800	1.074	4.259	42.628	65.599
850	1.123	10.876	62.856	66.453
900	5.630	13.688	63.199	69.103
950	0.533	6.071	22.857	65.028
1000	0.320	0.773	22.057	52.179
1050	0.237	0.204	21.600	39.873
1100	0.368	0.293	22.599	41.726

TABLE 6. Peak Temperature and Cooling Rate Effect on Furnace-Induced Sensitization for Type 304 SS Heat SS7

Peak Temperature, °C	Degree of Sensitization, C/cm²			
	1	2	3	4
800	6.133	6.243	41.701	43.173
850	7.000	14.685	42.723	45.709
900	8.293	22.608	45.892	48.178
950	6.823	11.370	24.685	44.228
1000	5.409	5.630	16.457	32.183
1050	0.021	0.810	14.207	20.105
1100	0.329	0.987	19.365	37.318

TABLE 7. Peak Temperature and Cooling Rate Effect on Furnace-Induced Sensitization Development for Type 316 SS Heat SS16

Peak Temperature, °C	Degree of Sensitization, C/cm²			
	1	2	3	4
800	0.000	0.765	14.105	28.042
850	0.000	6.961	27.290	35.343
900	0.368	8.293	42.723	62.196
950	1.279	10.708	30.514	67.428
1000	0.442	5.630	25.600	9.347
1050	0.000	0.000	2.760	5.185
1100	0.000	0.000	4.339	8.095

TABLE 8. Peak Temperature and Cooling Rate Effect on Furnace-Induced Sensitization Development for Type 316 SS Heat SS17

Peak Temperature, °C	Degree of Sensitization, C/cm²			
	1	2	3	4
800	0.000	2.857	32.400	51.745
850	0.442	14.304	51.002	70.687
900	0.464	16.783	77.679	82.336
950	5.331	27.707	52.457	58.285
1000	8.885	16.586	45.942	13.962
1050	0.000	0.000	3.168	7.936
1100	0.000	0.000	3.915	8.885

TABLE 9. Sensitization Development for Type 316 SS Heat SS16 Specimens Exposed to Gleeble Treatment Cycles

Temperature, °C	Heating Rate, °C/s	Holding Time, min	Cooling Rate, °C/s	DOS, C/cm²
950	2	0	2	4.06
	50	0	2	0.82
	2	15	2	0.00
	50	15	2	0.52
	2	0	0.05	68.00
	50	0	0.05	59.31
	2	15	0.05	81.14
	50	15	0.05	70.97
	50	0	1	4.46
	50	0	0.1	35.09
1000	2	0	2	2.29
	50	0	2	0.00
	2	15	2	0.00
	50	15	2	0.00
	2	0	0.05	72.00
	50	0	0.05	63.89
	2	15	0.05	68.57
	50	15	0.05	57.03
	50	30	0.05	8.34
	50	0	0.1	36.34
	50	0	1	1.66
1050	2	0	2	0.00
	50	0	2	0.00
	2	15	2	0.00
	50	15	2	0.00
	2	0	0.05	8.57
	50	0	0.05	0.00
	2	15	0.05	6.63
	50	15	0.05	5.60
	50	0	0.1	0.05
	50	0	1	0.00

TABLE 10. Peak Temperature and Cooling Rate Effect on Gleeble Induced Sensitization Development for Type 316 SS Heat SS16 at Heating Rate of 50°C/s and Zero Holding Time

Temperature, °C	Cooling Rate, °C/s			
	2	1	0.1	0.05
	Degree of Sensitization, C/cm²			
950	0.82	4.46	35.09	59.31
975	0.58	5.71	35.09	59.73
1000	0.00	1.66	36.34	63.89
1050	0.00	0.00	0.054	0.00

8.0 FIGURES

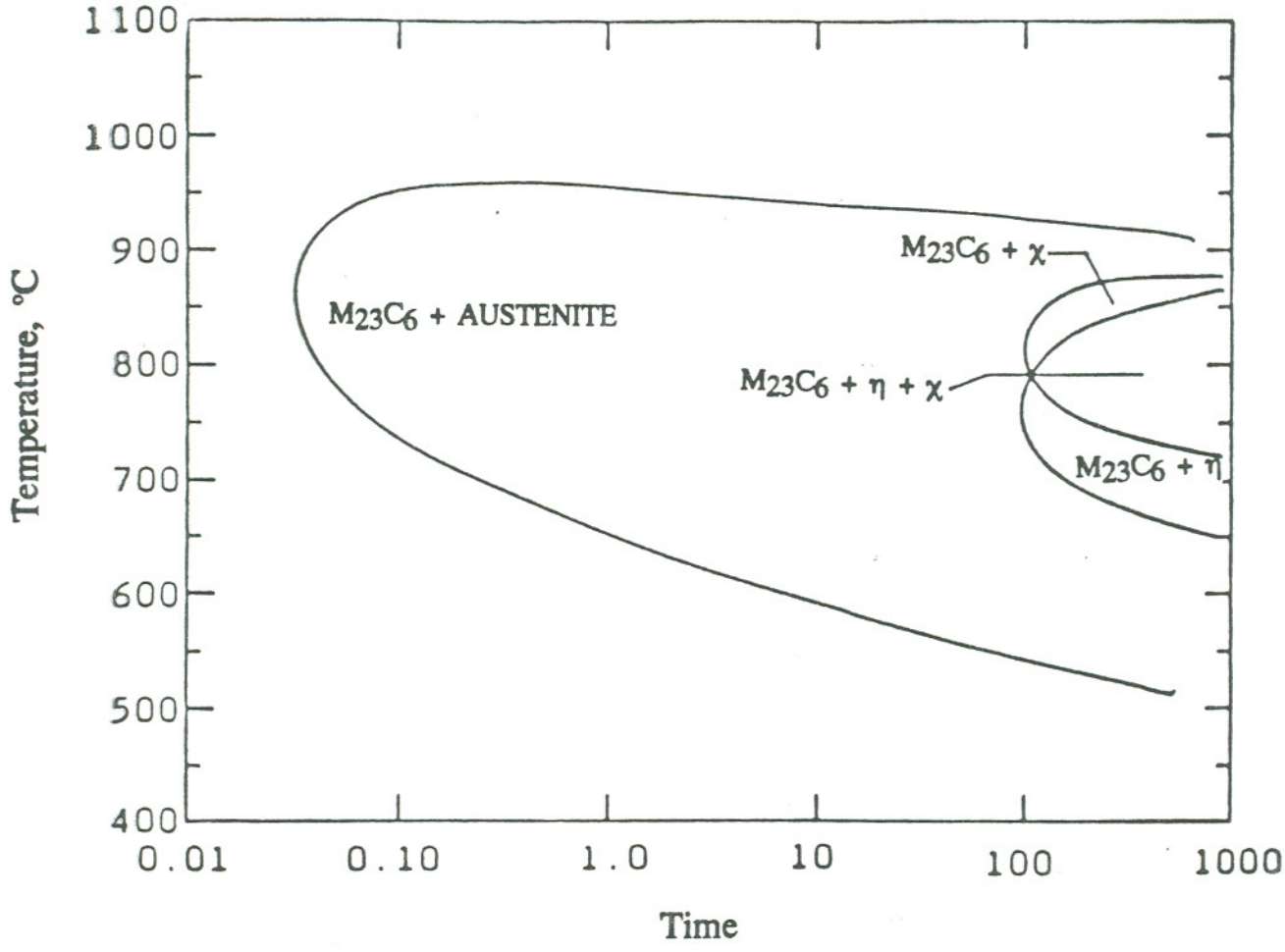

FIGURE 1. Typical Time-Temperature-Precipitation Diagram of High Carbon Type 316 SS Solution-Treated at 1260°C for 1.5 Hours and Water Quenched. (After Weiss and Stickler.[21])

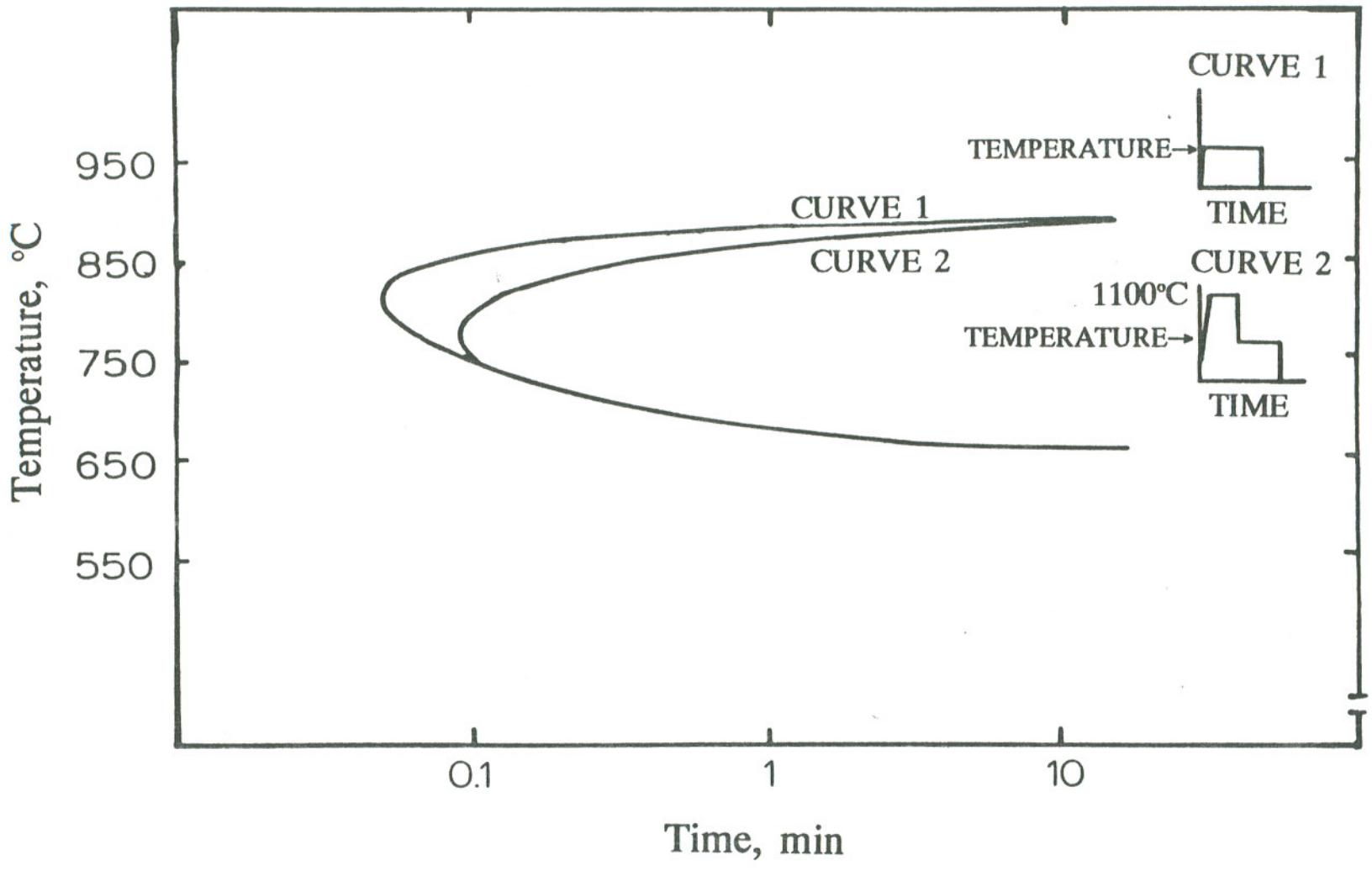

FIGURE 2. Change of $M_{23}C_6$ Precipitation Kinetics due to Pre-Isochemical Hold Temperature Cycles for a 0.05% Type 304. (After Ikawa et al.[22])

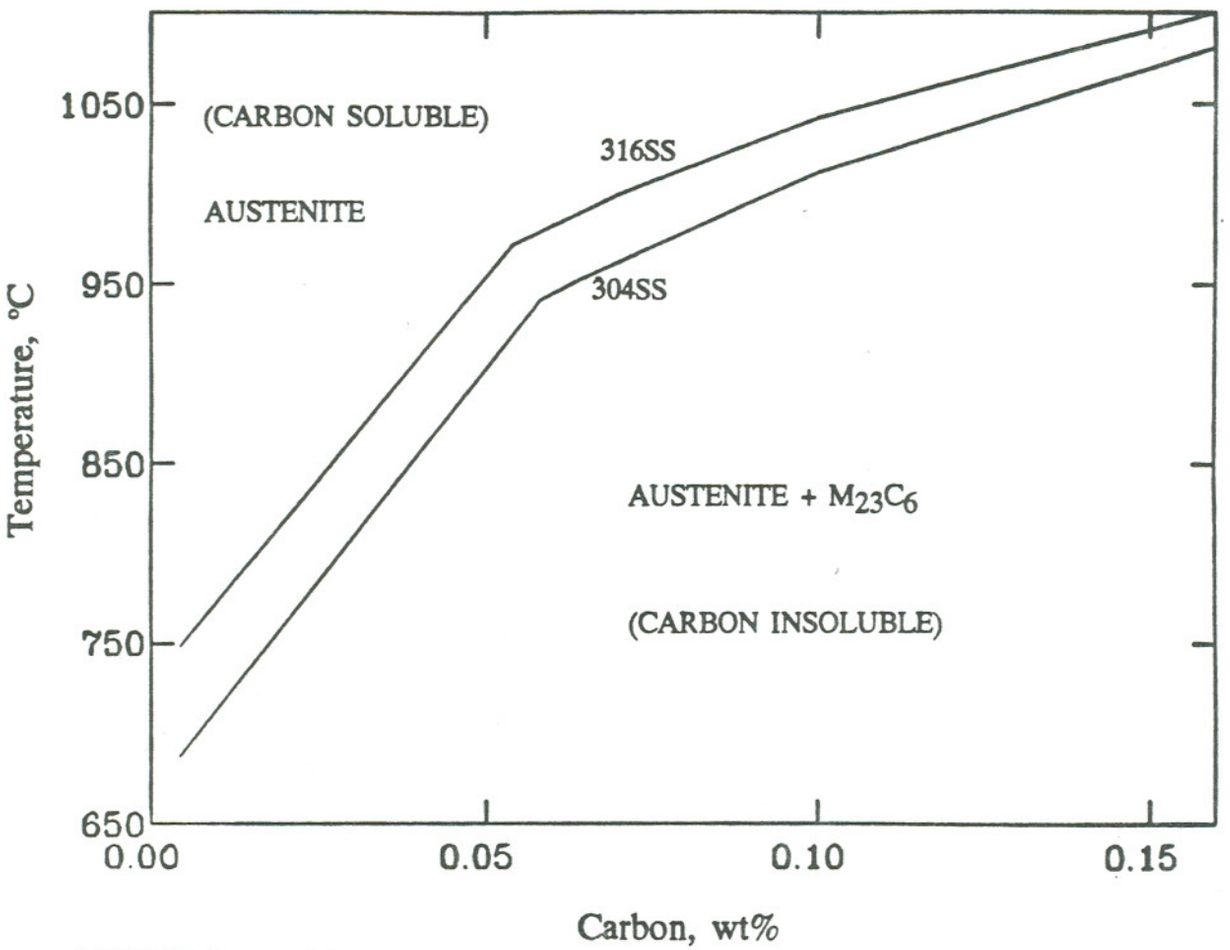

FIGURE 3. Variation of Carbon Solubility as a Function of Temperature and Carbon Content for Type 304 and 316 SSs.

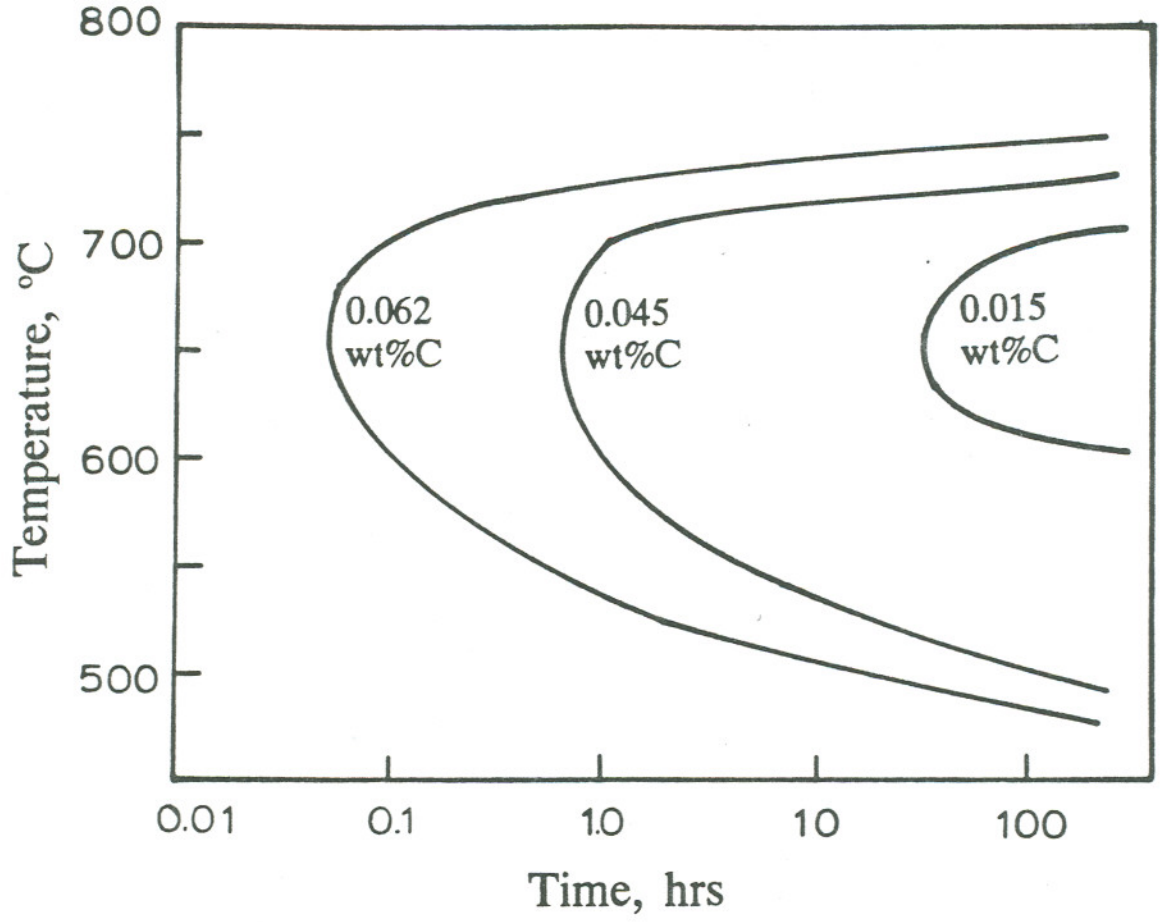

FIGURE 4. Time-Temperature-Sensitization (initiation) Curves for Type 304 SSs with Various Carbon Contents. (After Bruemmer et al.[2])

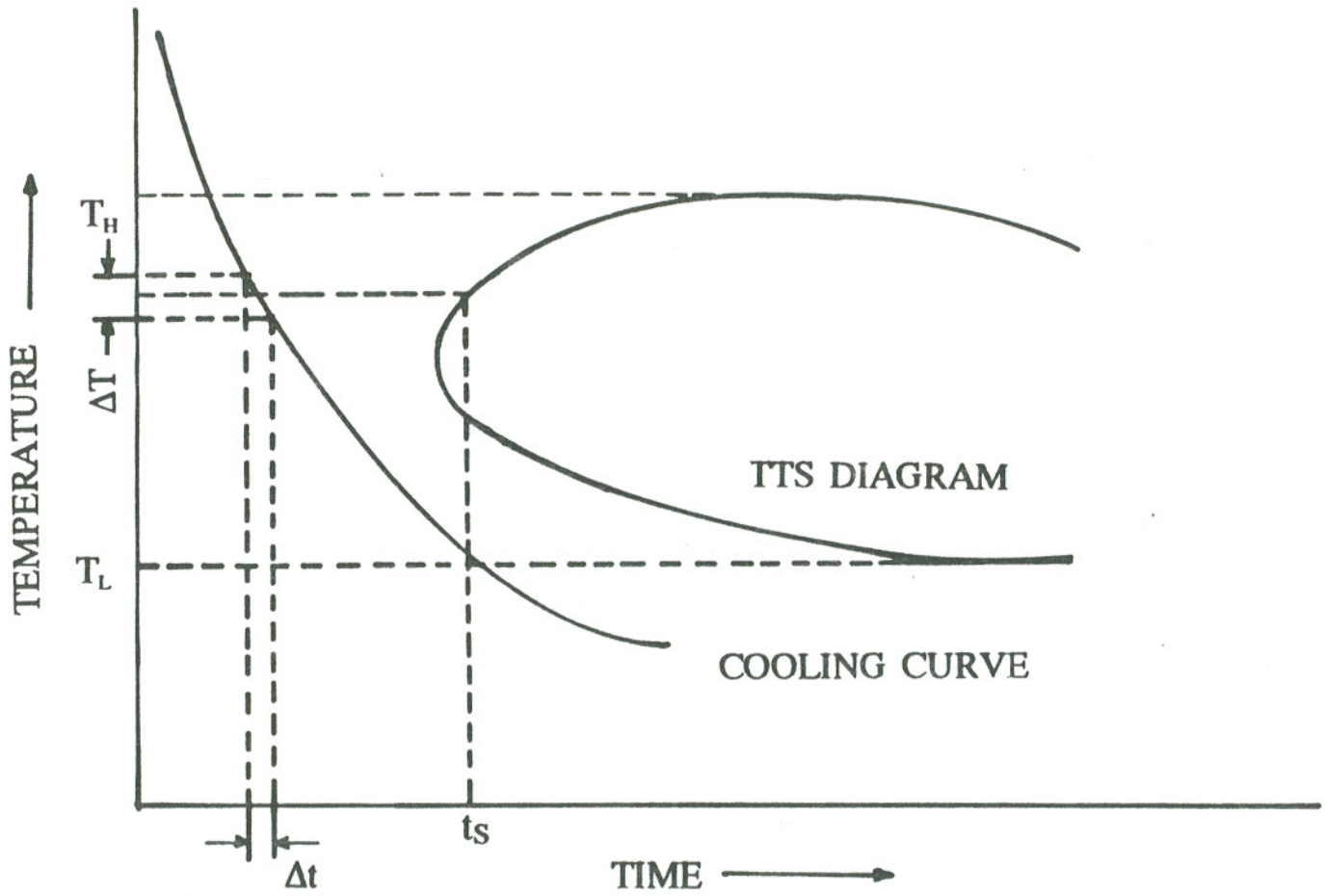

FIGURE 5. Schematic Illustration of the Application of the Mannig-Loring Method to Prediction of the Presence of Sensitization due to a Continuous Cooling Cycle. (After Dayal and Gnanmoorthy.[28])

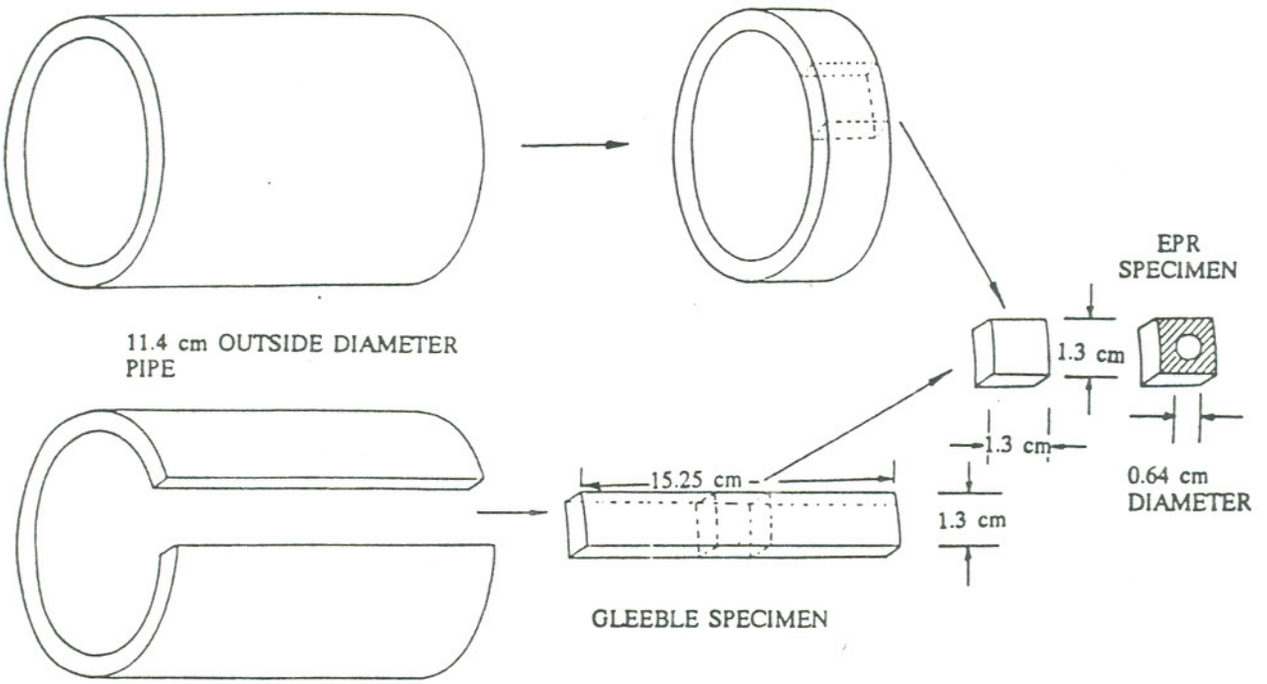

FIGURE 6. Schematic of Sequence for Pipe Material to be Used as Gleeble Specimen and Then Subsequently as an EPR Specimen.

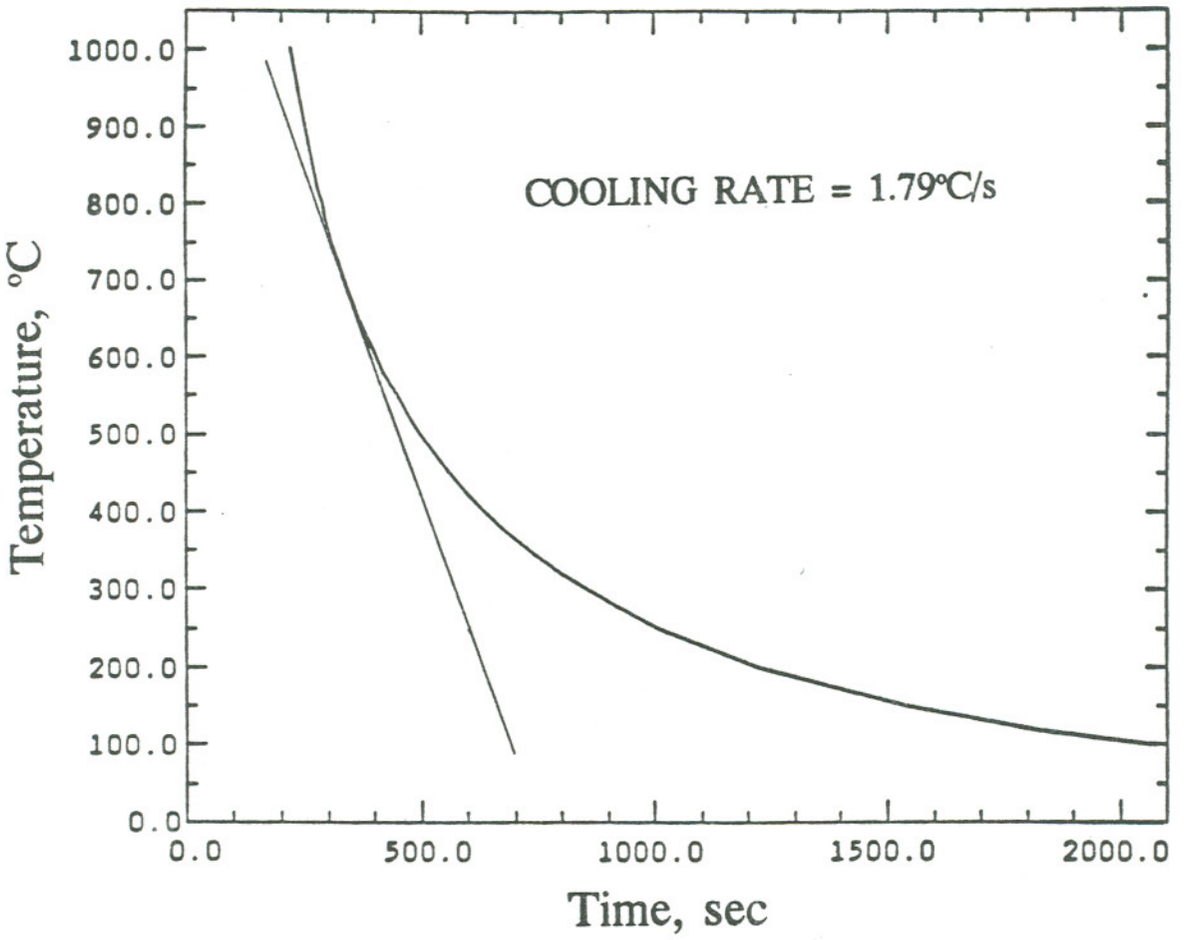

FIGURE 7. Typical Continuous Cooling Curve for Specimen Heat Treated to a Peak Temperature of 1000°C in the Furnace and Subsequently Cooled at 1.8°C/s.

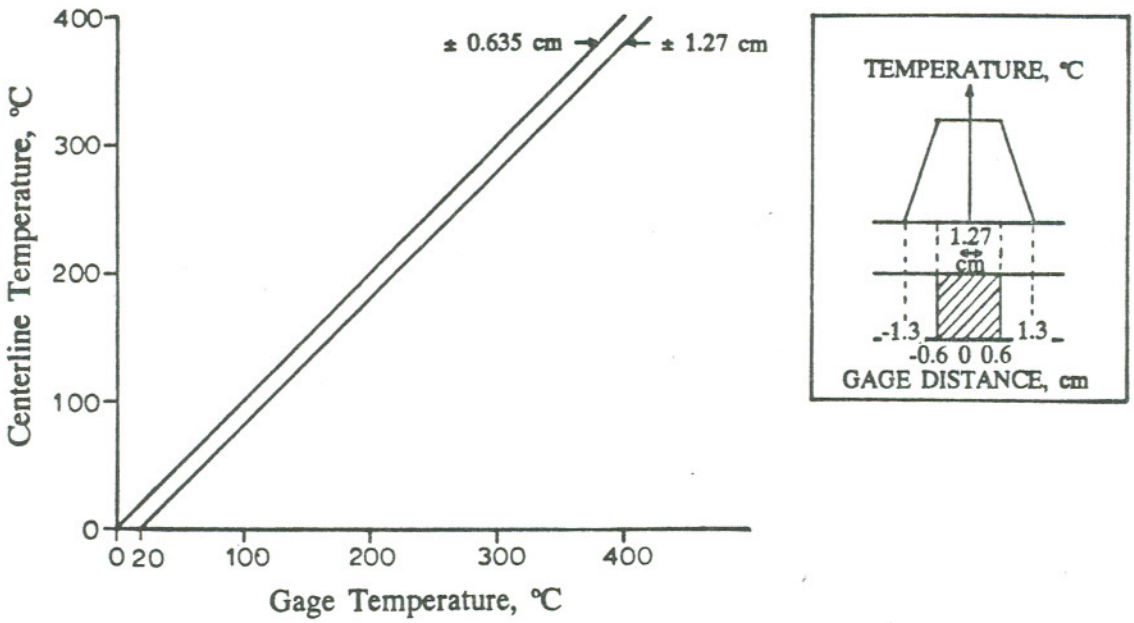

FIGURE 8. Gleeble Heated SS Gage Section Temperature Gradient Profile.

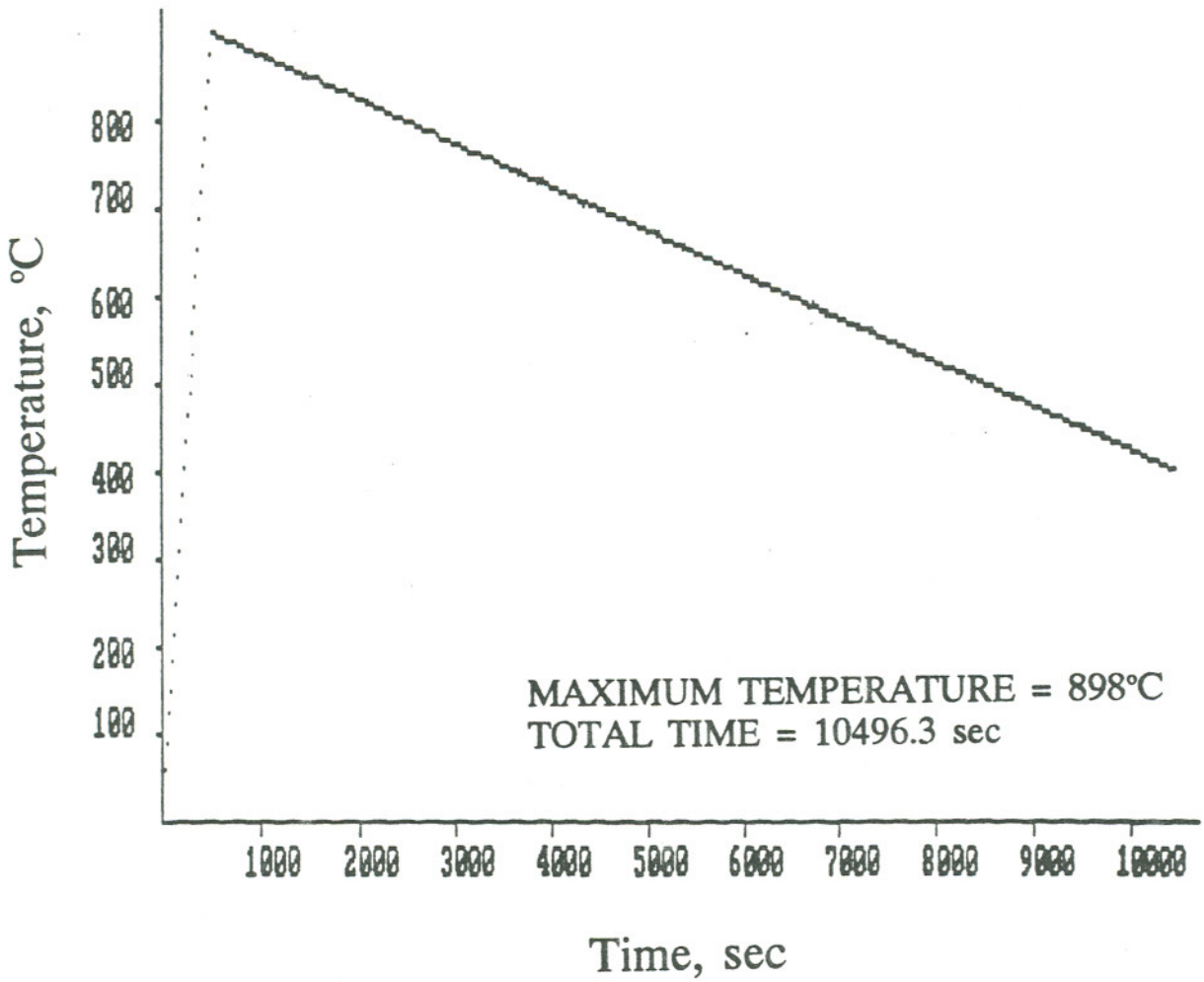

FIGURE 9. Typical Heating and Cooling Cycle for Specimens Heat Treated in the Gleeble.

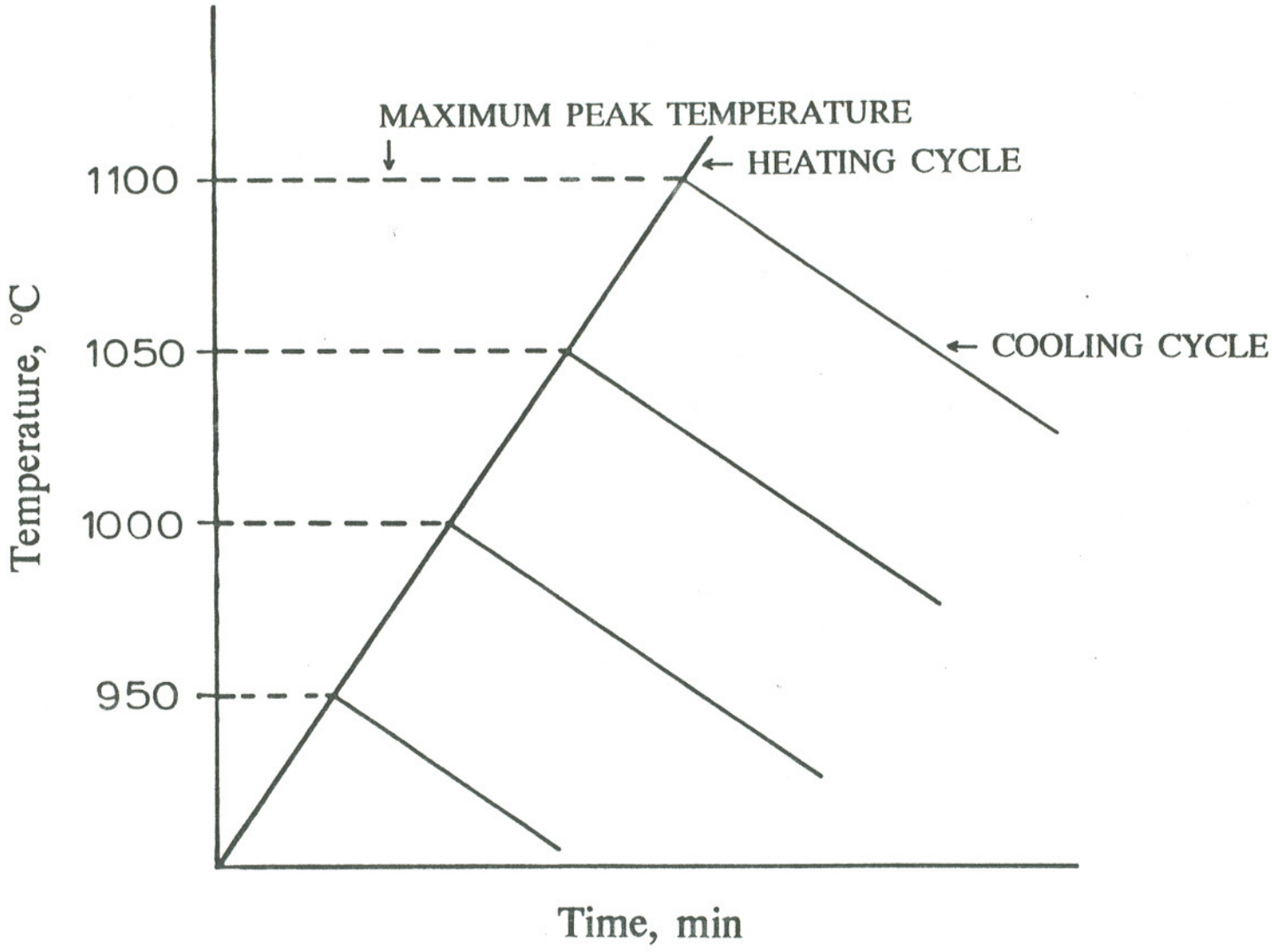

FIGURE 10. Schematic of the Heating and Cooling cycles for Specimens Heat Treated in the Gleeble.

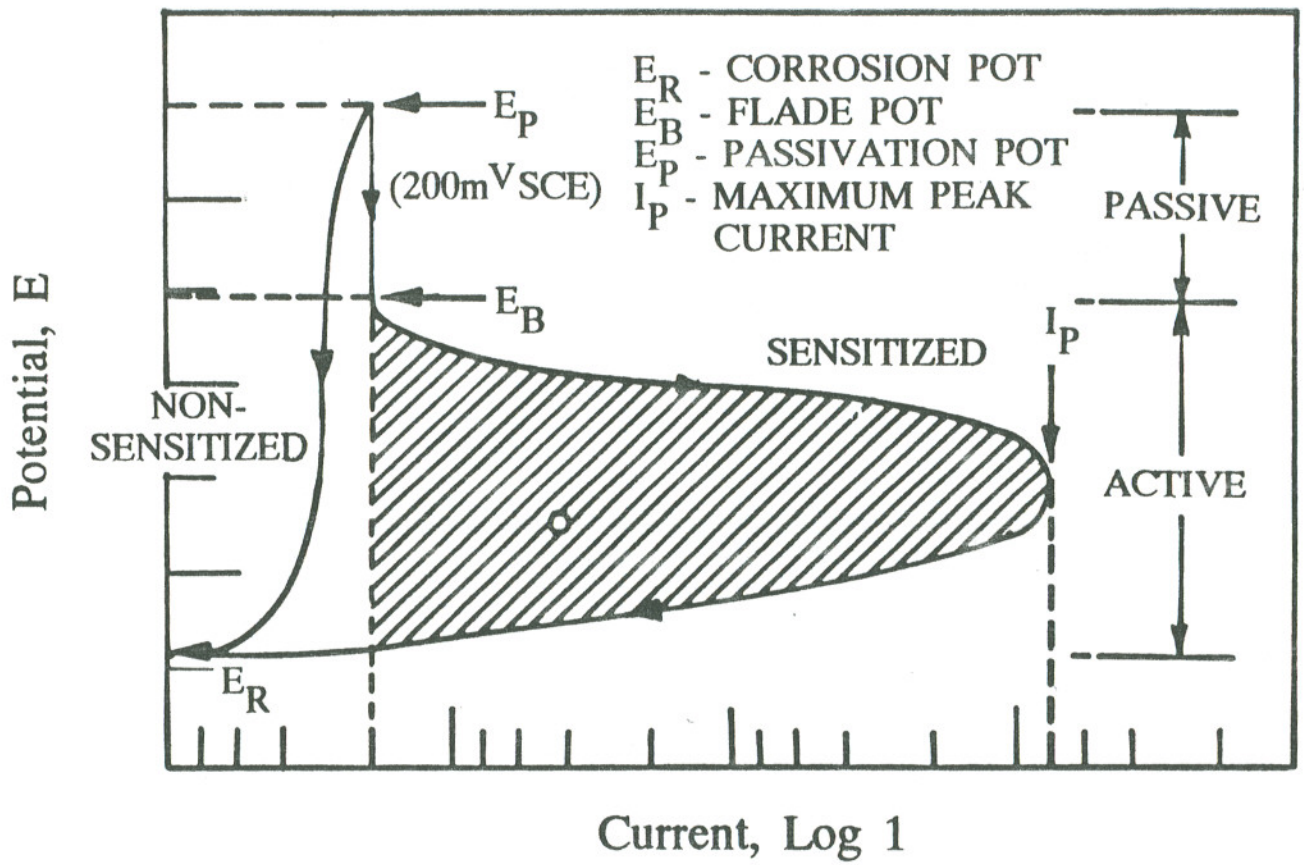

FIGURE 11. Schematic of EPR Test Illustrating Material Response for a Sensitized and Non-Sensitized Specimen.

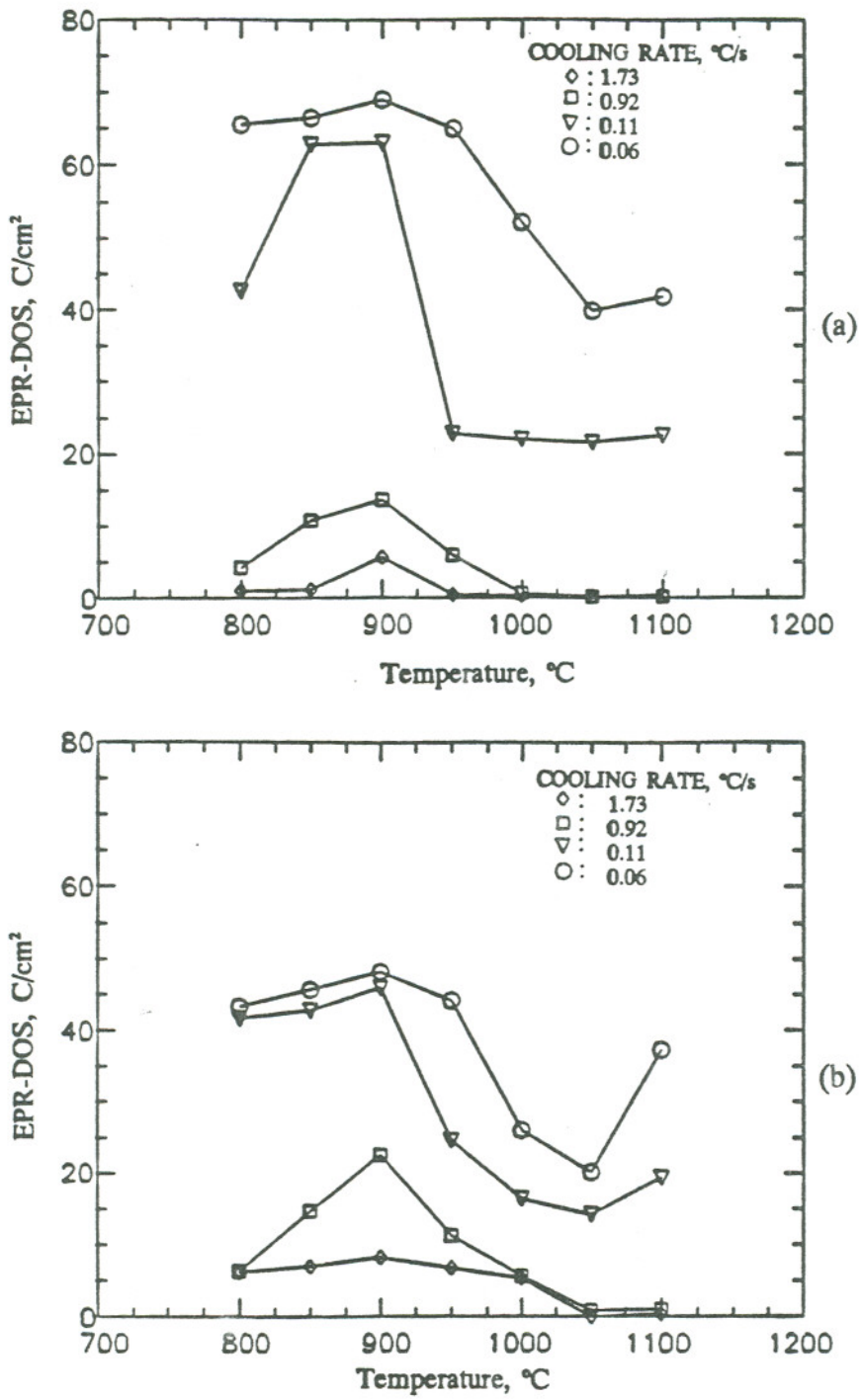

FIGURE 12. Sensitization Development for Austenitic Type 304 SS [(a) Heat SS6; (b) Heat SS7] as a Function of Peak Temperature and Cooling Rate during Continuous Cooling Heat Treatment.

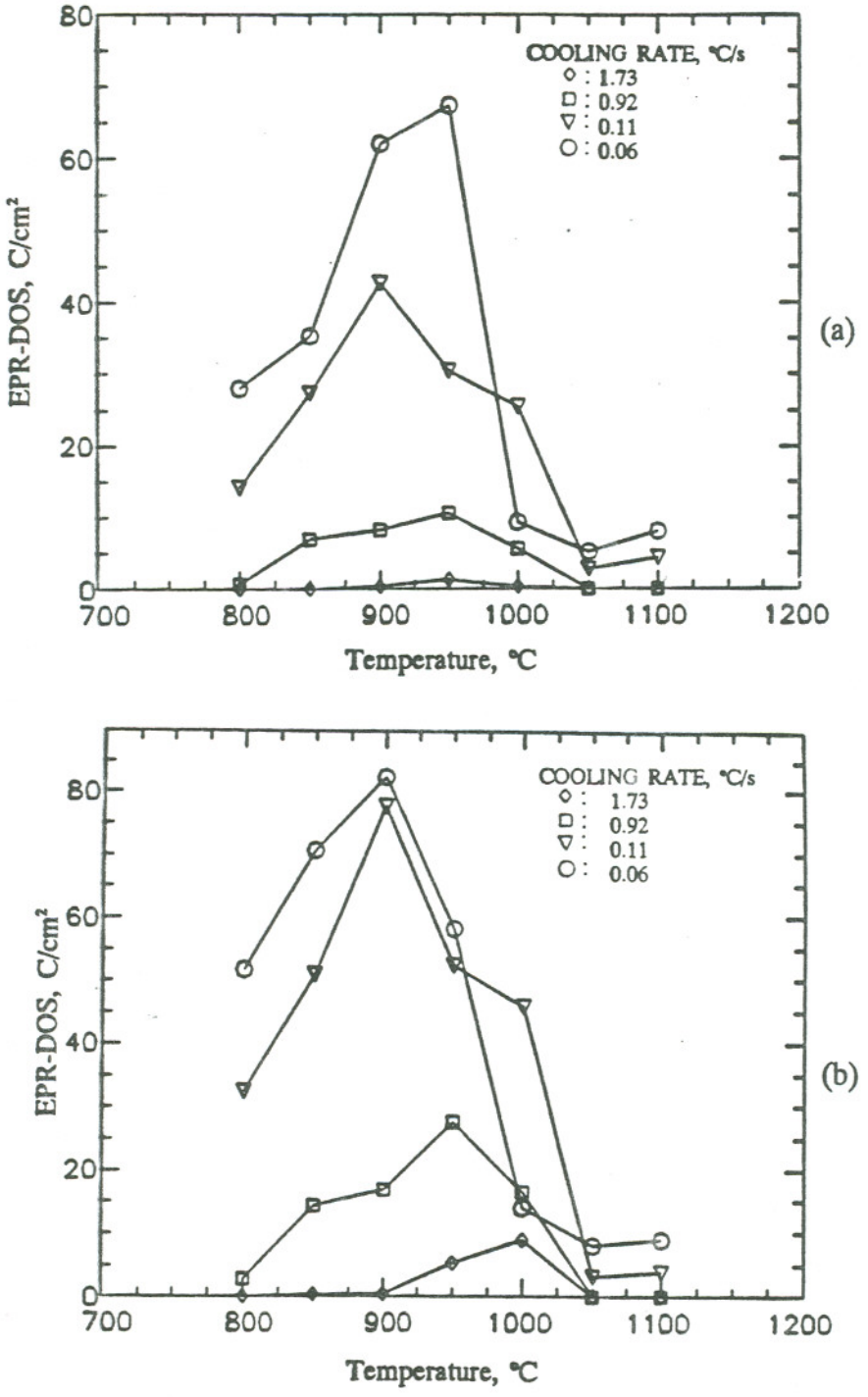

FIGURE 13. Sensitization Development for Type 316 SS [(a) Heat SS16; (b) Heat SS17) as a Function of Peak Temperature and Cooling Rate during Continuous Cooling Heat Treatment.

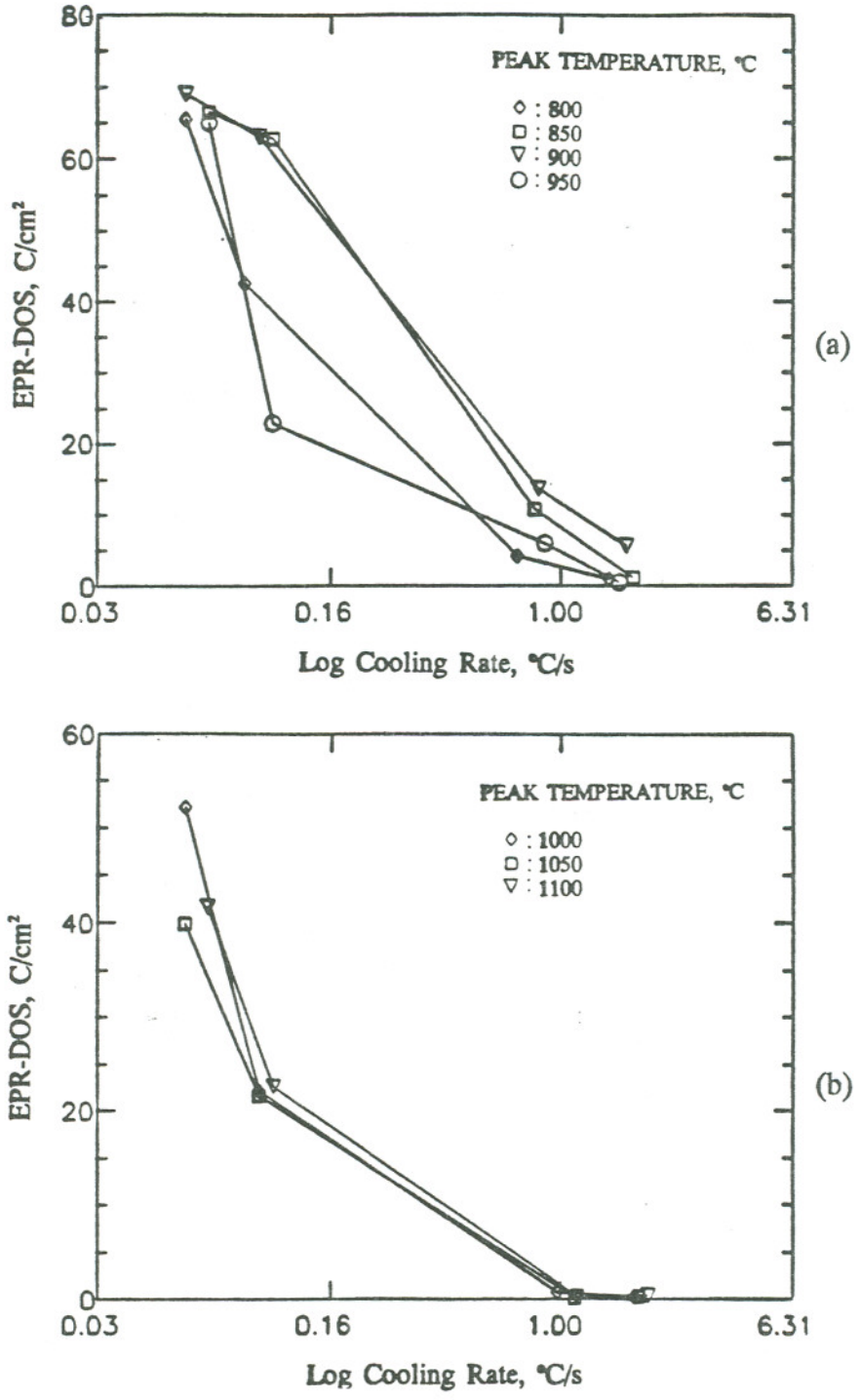

FIGURE 14. Sensitization Development for Type 304 SS Heat SS6 as a Function of Cooling Rate and Peak Temperature during Continuous Cooling Rate Heat Treatment.

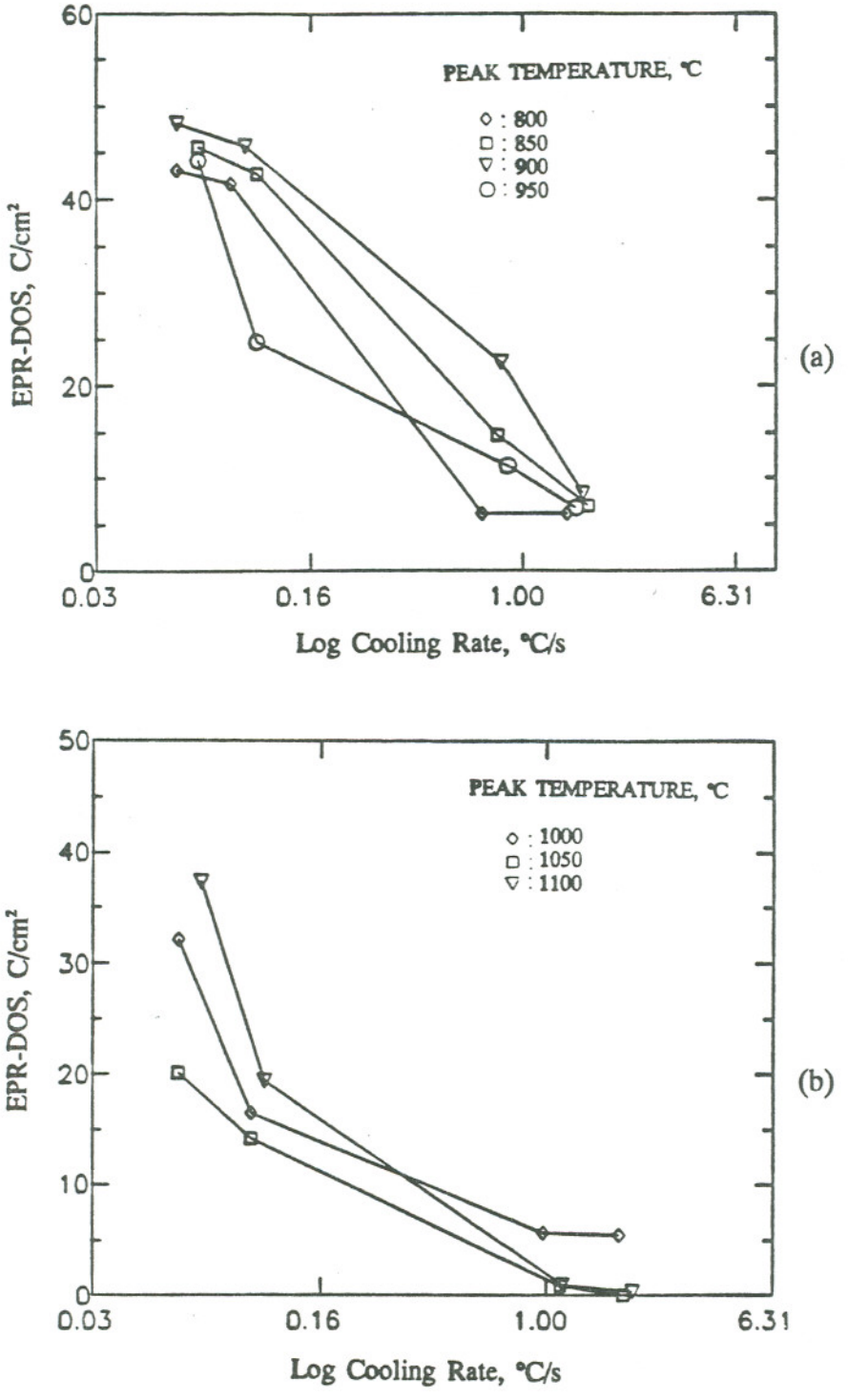

FIGURE 15. Sensitization Development for Type 304 SS Heat SS7 as a Function of Cooling Rate and Peak Temperature during Continuous Cooling Rate Heat Treatment.

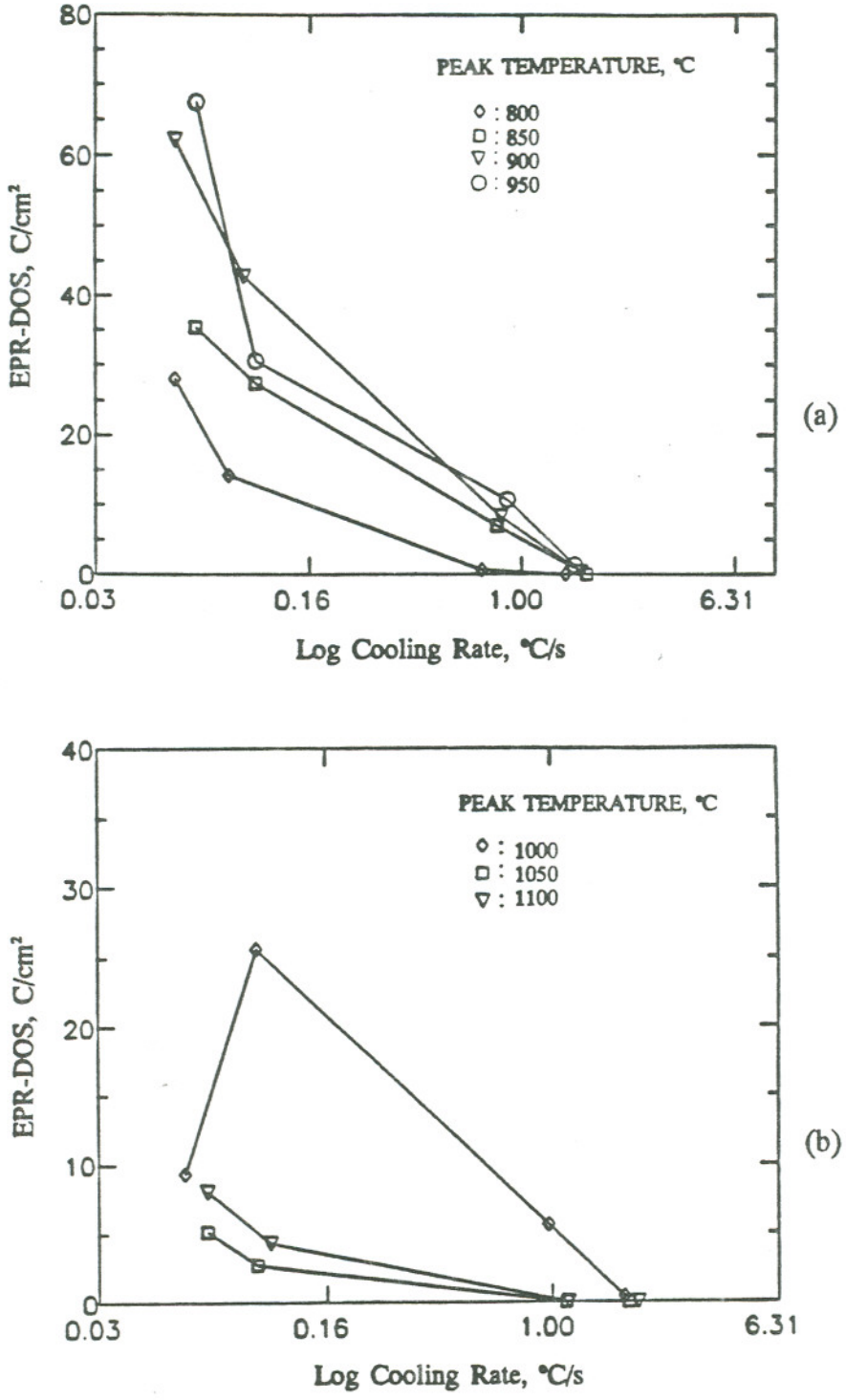

FIGURE 16. Sensitization Development for Type 316 SS Heat SS16 as a Function of Cooling Rate and Peak Temperature during Continuous Cooling Rate Heat Treatment.

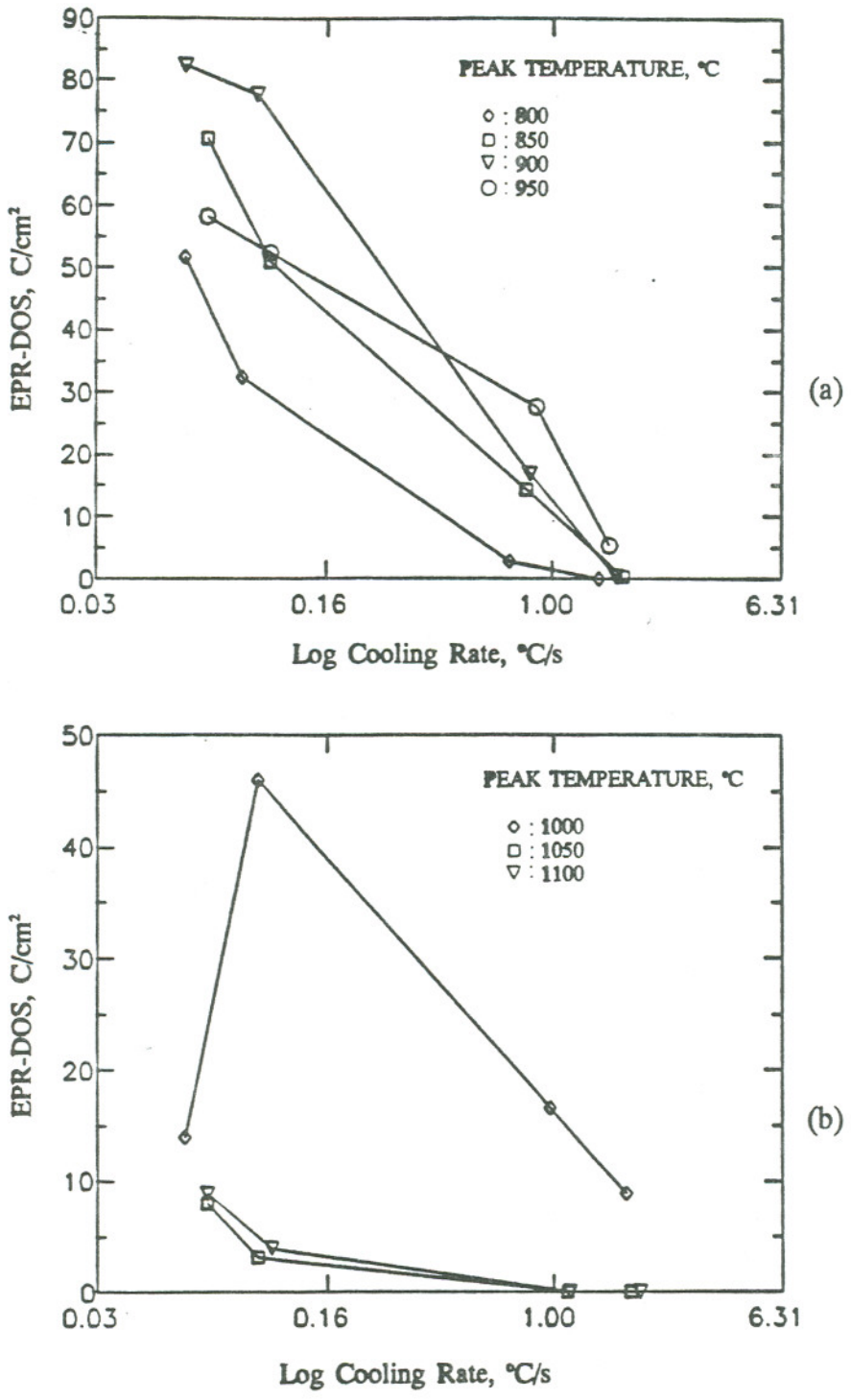

FIGURE 17. Sensitization Development for Type 316 SS Heat SS17 as a Function of Cooling Rate and Peak Temperature during Continuous Cooling Rate Heat Treatment.

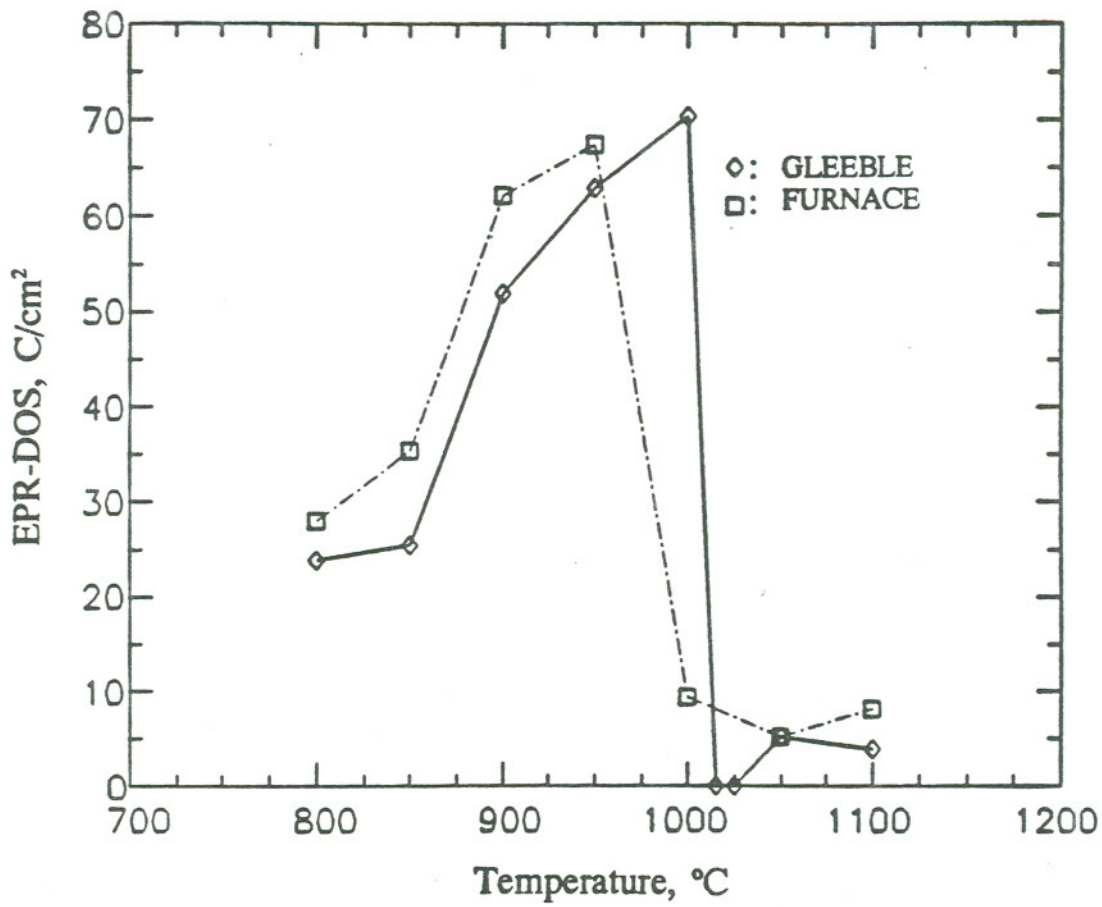

FIGURE 18. Comparison of EPR-DOS Values for Type 316 SS Heat SS16 Exposed to Furnace and Gleeble Thermal

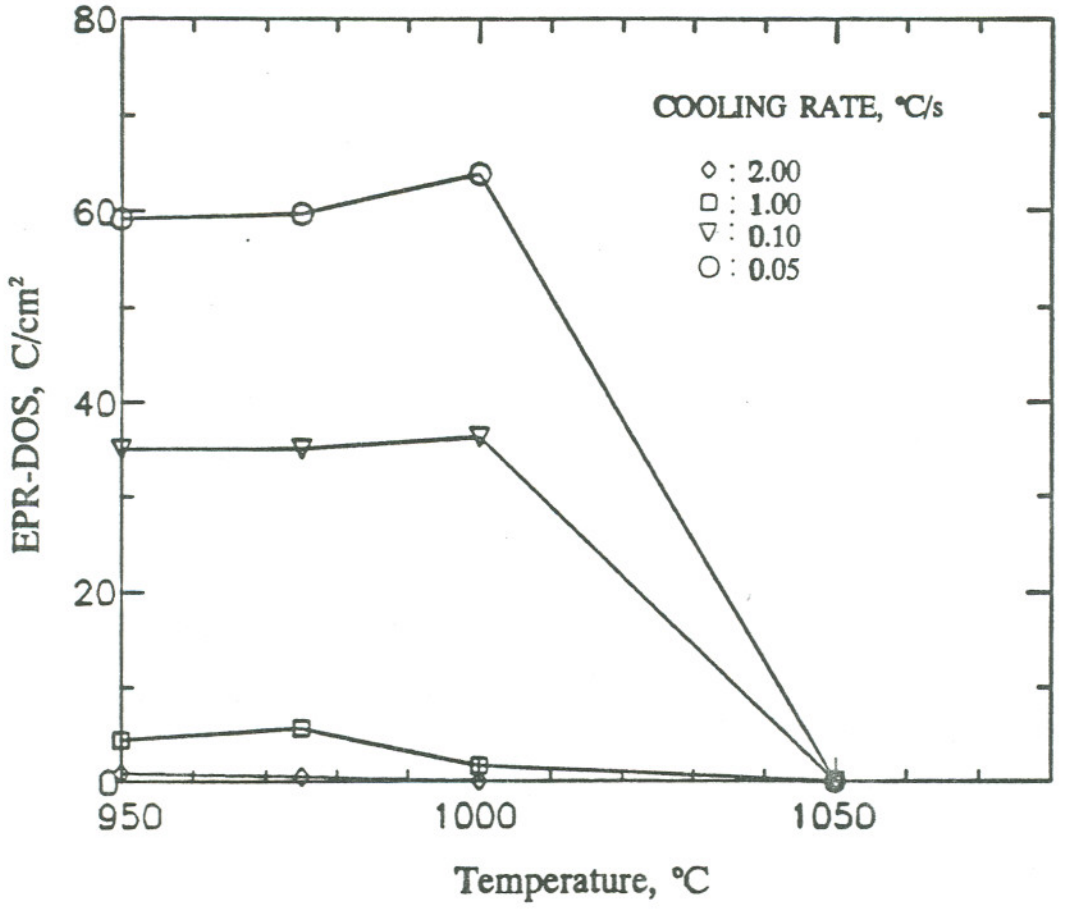

FIGURE 19. Peak Temperature and Cooling Rate Effect on Sensitization for Type 316 SS Heat SS16 at a Heating Rate of 50°C/s and Zero Holding Time.

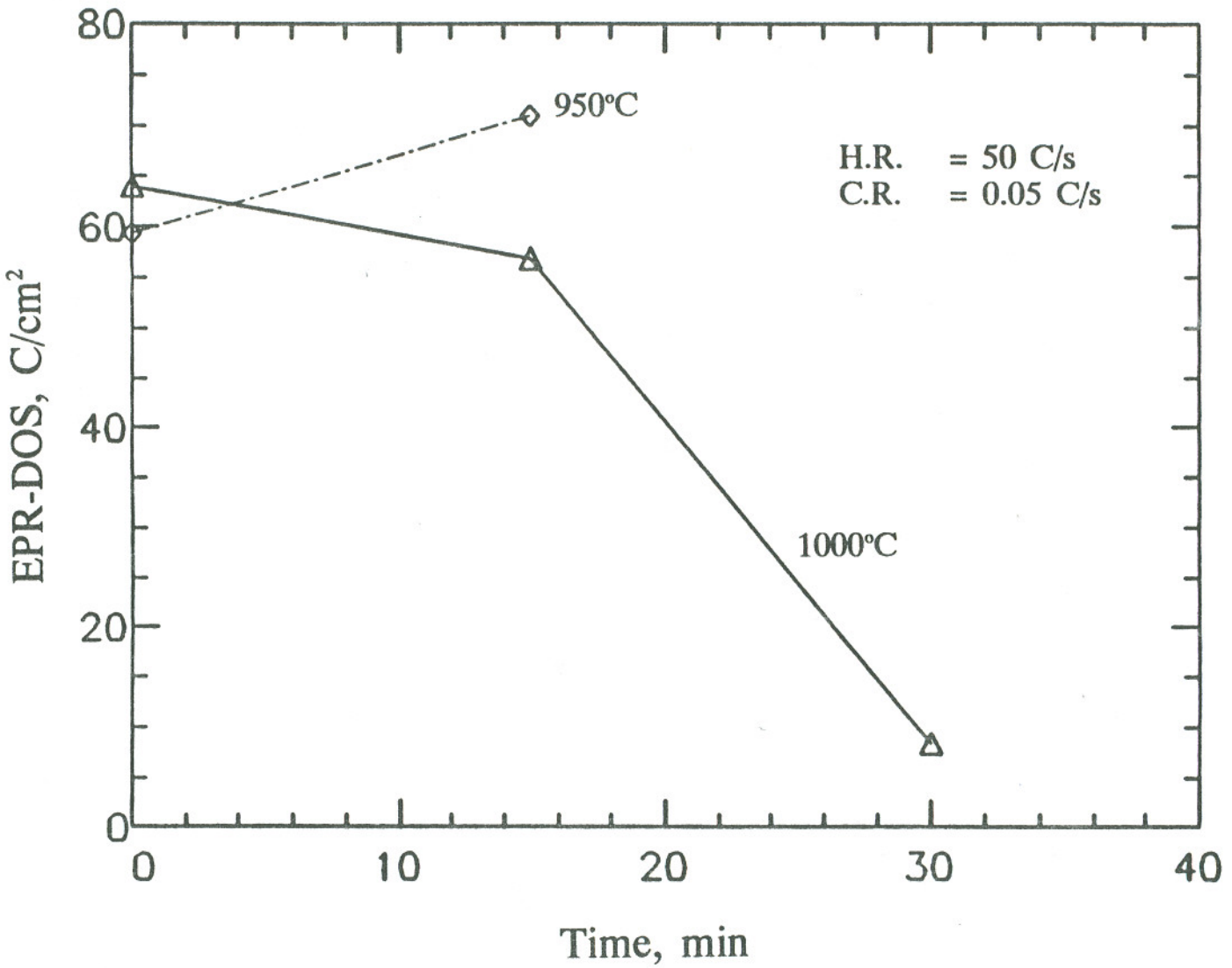

FIGURE 20. Effect of Peak Temperature Holding Time on Subsequent Sensitization Development.

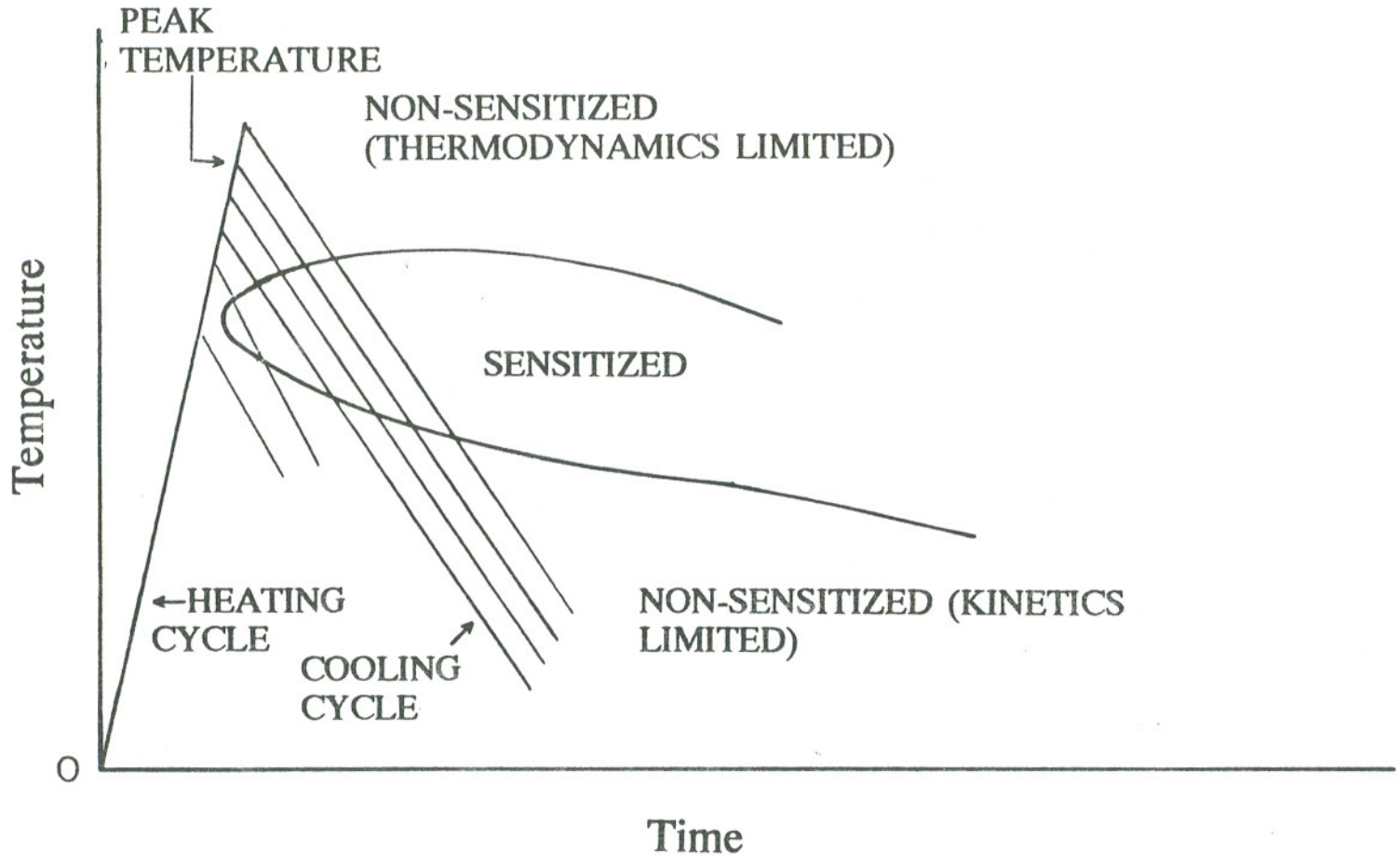

FIGURE 21. Schematic Illustration of Effect of Peak Temperature Achieved on Sensitization Development.

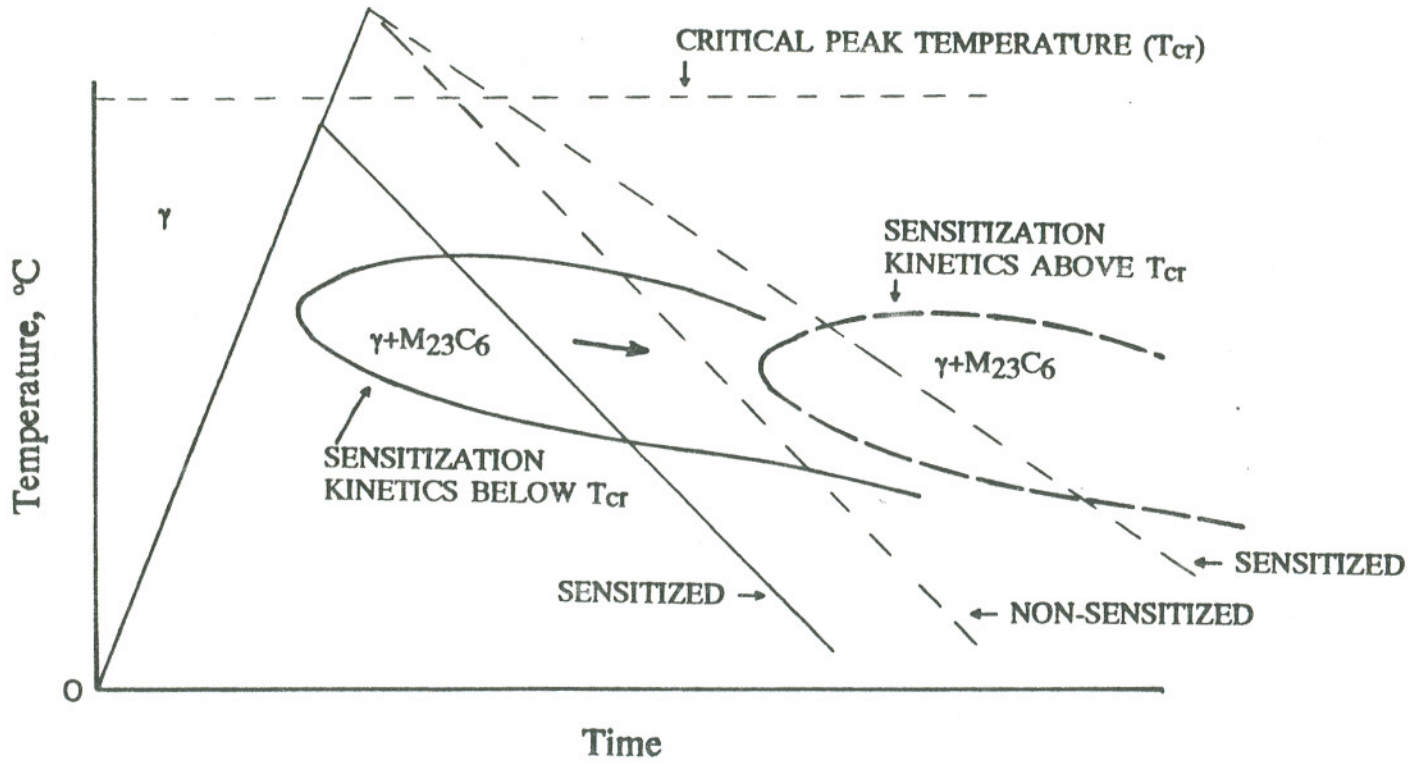

FIGURE 22. Schematic Illustration of Change in Sensitization Kinetics with Increasing Peak Temperature.

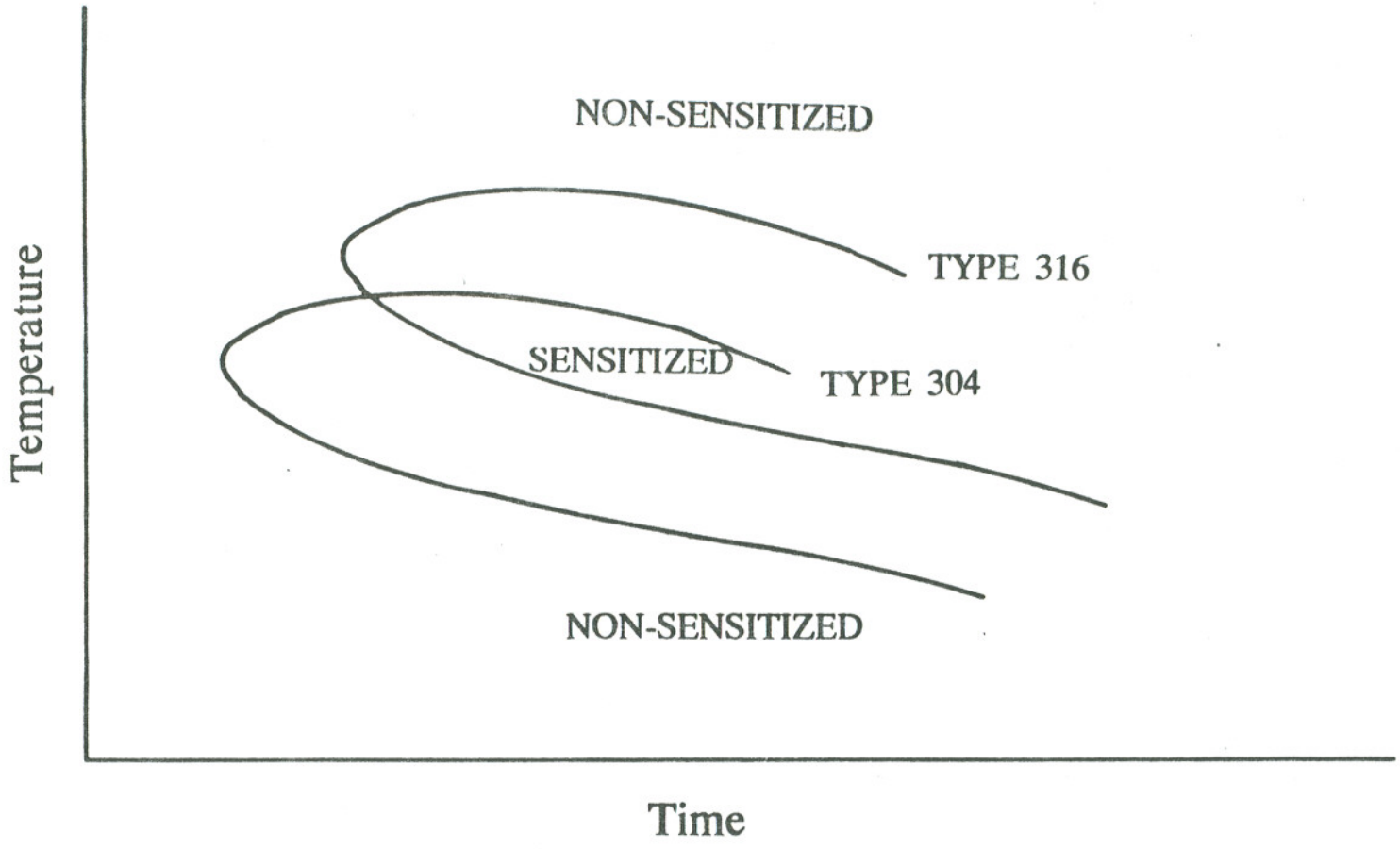

FIGURE 23. Schematic TTS Curves for Type 304 and 316 SS.

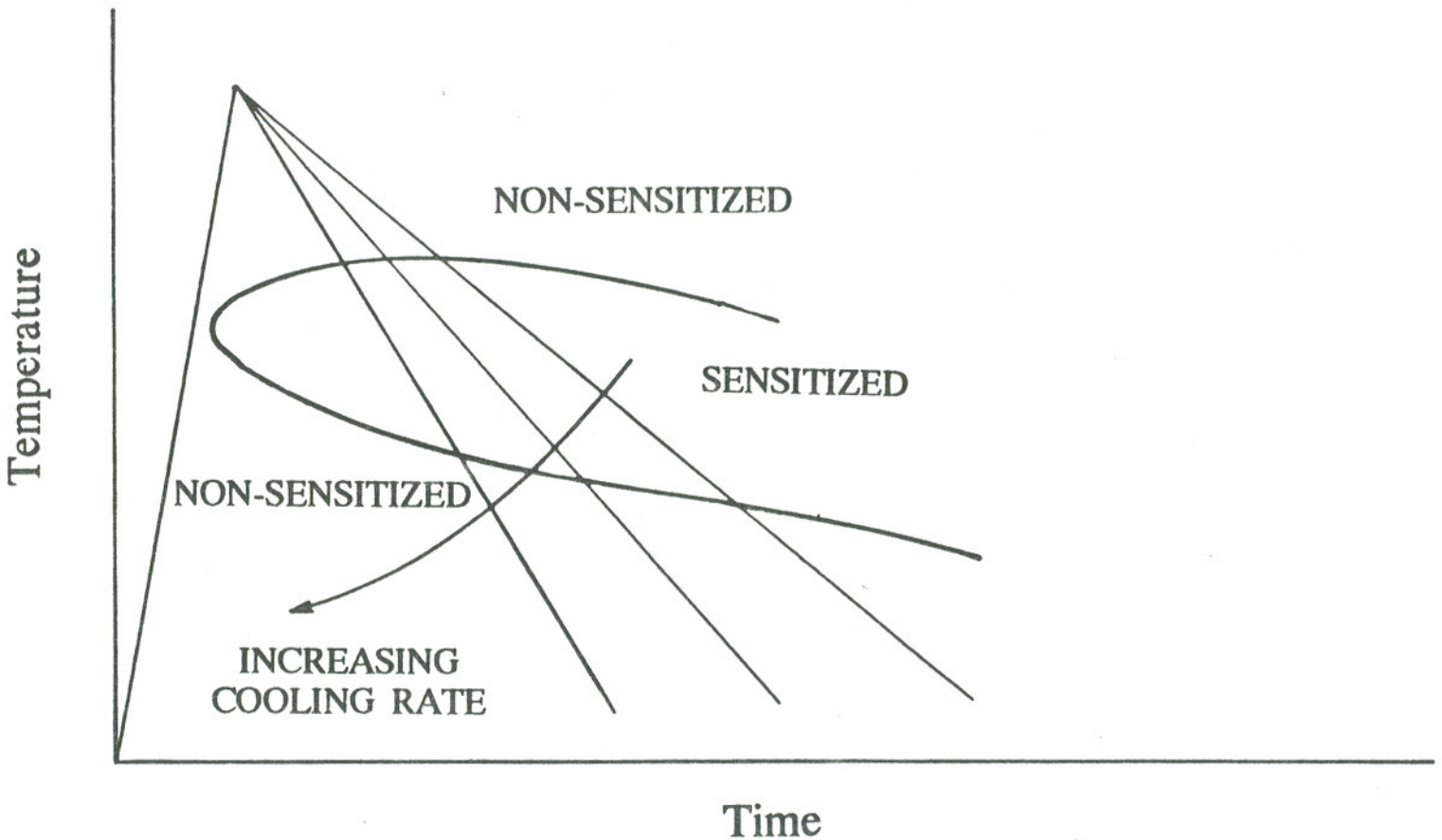

FIGURE 24. Schematic Illustration of Cooling Rate Effect on Sensitization Development during Thermal Cycles.

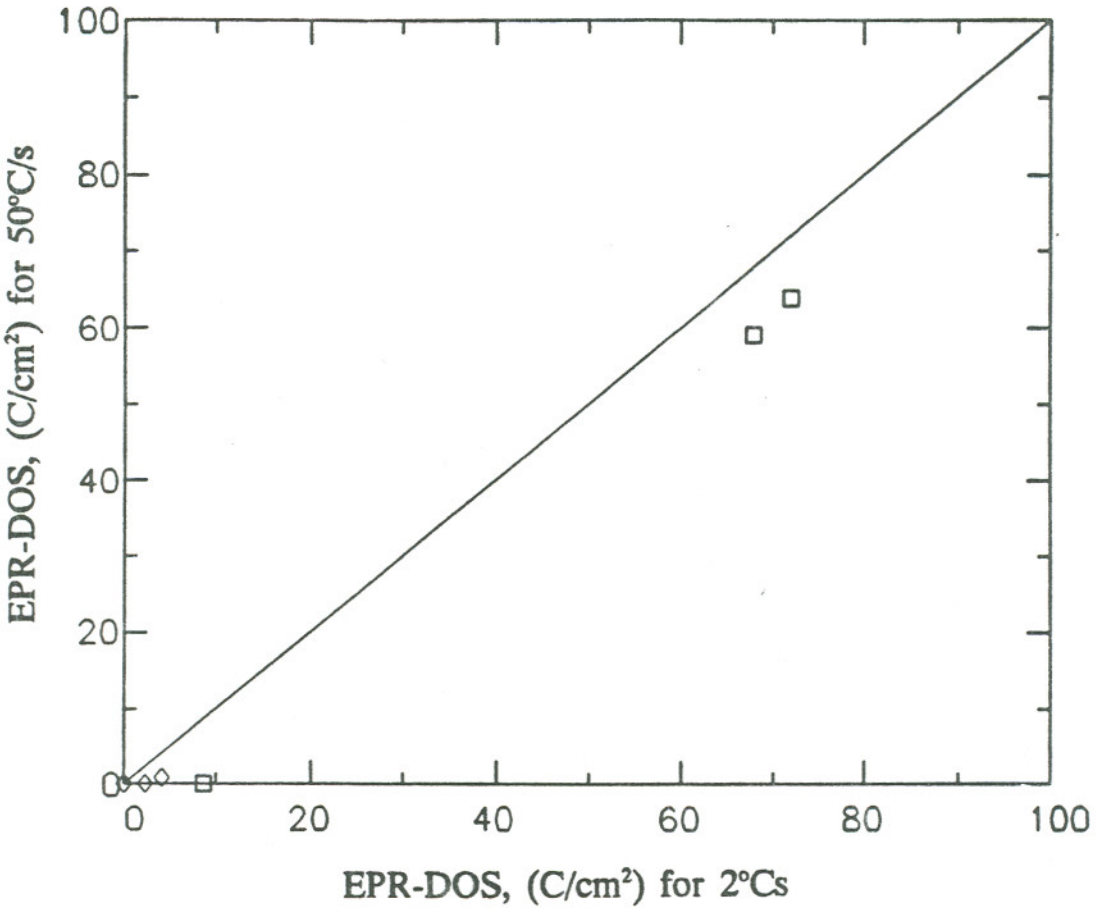

FIGURE 25. Correlation Between EPR-DOS for Specimens Subjected to a Heating Rate of Either 2 or 50°C/s, Peak Temperatures Between 950 and 1050°C and a Cooling Rate of 2°C/s.

9.0 REFERENCES

1. S. M. Bruemmer, "Quantitative Measurement and Modeling of Sensitization Development in Stainless Steels," Doctor of Philosophy in Materials Science and Engineering Thesis, Oregon Graduate Center, Beaverton OR, May 1988.
2. D. G. Atteridge and S. M. Bruemmer, "Evaluation of Weld and Repair-Welded Stainless Steel for Light Water Reactor (LWR) Service," U.S. Nuclear Regulatory Commission, NUREG/CR-3613, PNL-4941, Vol. 3, No. 2, Published, Oct 1986.
3. S. M. Bruemmer, L. A. Charlot, and D. G. Atteridge, "Evaluation of Welded and Repair-Welded Stainless Steel for Light Water Reactor (LWR) Service," Compositional Effects on the Sensitization of Austenitic Stainless Steels, U.S. Nuclear Regulatory Commission, NUREG/CR-3918, PNL-5186, Published, Dec 1987.
4. S. M. Bruemmer, L. A. Charlot, and D. G. Atteridge, "Sensitization Development in Austenitic Stainless Steel: II Measurement and Prediction of Thermomechanical History Effects," Submitted for Publication in Corrosion Journal, Dec 1986.
5. M. Hishida and H. Nakada, "Sensitization and Subsequent Intergranular Stress Corrosion Cracking in High Temperature Water," Corrosion Journal, Vol. 34, No. 10, Oct 1984.

6. E. A. Loria, "Evaluating Tendency for Sensitization in Type 304 Stainless Steel via Jominy Bar Testing," Journal of Metal, p 137, June 1979.

7. E. A. Loria, "Studies of Fabrication-Related Sensitization in Type 304 Stainless Steel," Journal of Metal, p 163, Dec 1979.

8. H.D. Solomon, "Continuous Cooling Sensitization of Type 304 Stainless Steel," Corrosion Journal, Vol. 34, No. 6, p 183, June 1978.

9. H. D. Solomon, "The influence of Prior Deformation on Continuous Cooling Sensitization of Type 304 Stainless Steel," Corrosion Journal, Vol. 36, No. 7, p 356, July 1980.

10. H. D. Solomon, "Influence of Composition on Continuous Cooling Sensitization of Type 304 Stainless Steel," Corrosion Journal, Vol. 40, No. 2, p 51, Feb 1984.

11. H. D. Solomon and D. C. Lord, "Influence of Strain During Continuous Cooling on the Sensitization of Type 304 Stainless Steel," Vol. 36, No. 8, p 395, Aug 1980.

12. E. C. Bain, R. H. Auborn, J. J. Rutherford, Trans. Amer. Soc. Steel Treaters, Vol. 21, No. 6, p 481, 1933.

13. C. Strastrom and M. Hillert, "An Improved Depleted-Zone Theory of Intergranular Corrosion of 18-8 Stainless Steel," Journal of The Iron Institute, Vol. 207, No. 1, p 77, 1969.

14. C. S. Tedmon, Jr., D. A. Vermilye, and J. H. Rosolowski, "Intergranular Corrosion of Austenitic Stainless Steel," Vol. 118, No. 2, p 192, 1971.

15. L. K. Singhal and J. W. Martin, "The Growth of $M_{23}C_6$ Carbide on Grain Boundaries in an Austenitic Stainless Steel," Transactions of the Metallurgical Society of AIME, Vol. 242, p 814, May 1968.

16. C. Da Casa, V. B. Nielshwar, and D. A. Melford, "$M_{23}C_6$ Precipitation in Unstabilized Austenitic Stainless Steel," Journal of The Iron Steel Institute, p 1325, Oct 1969.

17. F. R. Becitt and B. R. Clark, "The Shape and Mechanism of Formation of $M_{23}C_6$ Carbide in Austenite," Acta Metallurgica, Vol. 15, p 113, Jan 1967.

18. M. H. Lewis and B. Hattersley, "Precipitation of $M_{23}C_6$ in Austenitic Steels," Acta Metallurgica, Vol. 13, p 1159, Nov 1965.

19. L. K. Singhal and J. W. Martin, "The Growth of $M_{23}C_6$ Carbide on Incoherent Twin Boundaries in Austenite," Acta Metallurgica, Vol. 15, p 1603, Oct 1967.

20. G. P. Airey, "Microstructural Aspects of the Thermal Treatments of Inconel Alloy 600," Metallograph an International Journal, Vol. 13, No. 1, p 21, Feb 1980.

21. B. Weiss and R. Stickler, "Phase Instabilities During High Temperature Exposure of 316 Austenitic Stainless Steel," Metallurgical Transactions, Vol. 13, p 851, Apr 1972.

22. H. Ikawa, Y. Nakao, and K. Nishimoto, "Study of Weld Decay in SUS 304 Precipitation Phenomena of $M_{23}C_6$ During Thermal Cycles," Technical Reports of Osaka University, No. 1434 p 369, 1978.

23. K. Natesan and T. F. Kassner, Nucl. Technol., Vol. 19, No. 46, 1973.

24. M. Deighton, "Solubility of $M_{23}C_6$ in Type 316 Stainless Steel," Journal of The Iron and Steel Institute, p 1012, 1970.

25. E. Loria, "Effect of Microalloying on Continuous Cooling Sensitization of Type 304 Stainless Steel," Corrosion Journal, Vol. 40, No. 8, p 441, 1984.

26. Source Book on Stainless Steels, Compiled by the Periodical Publication Department, American Society for Metal, p 32.

27. A. Bose and P. K. De, "An EPR Study on the Influence of Prior Cold Work on the Degree of Sensitization of AISI 304 Stainless Steel," Corrosion Journal, Vol. 43, No. 10, pp 624, Oct 1987.

28. R. K. Dayal and J. B. Gnanomoorthy, "Predicting Extend of Sensitization During continuous Cooling from Temperature-Time-Sensitization Diagram," Corrosion Journal, Vol. 36, No. 1, pp 104, Feb 1980.

29. A. M. Cottrell, An Introduction to Metallurgy, ELBS and Edward Arnorld (Publishers) Ltd. London, pp 374, 1975.

30. Annual Book of ASTM Standard, "Standard Practices for Detecting Susceptibility to Intergranular Attack in Austenitic Stainless Steels," Designation A262-86, (American Society for Testing Material, Philadelphia, PA), 1987.

31. W. L. Clark, et al, "Comparative Methods for Measuring Degree of Sensitization in Stainless Steel," Intergranular Corrosion of Stainless Steel Alloy, ASTM STP 656, R. F. Steigerwald, Editorial American Society for Testing and Material, 1978.

32. ASTM Book of Standards, Vol. 2.01, E112-85, ASTM, Philadelphia, Pennsylvania, p. 815, 1988.

33. C. L. Briant, R. A. Mulford, and E. L. Hall, "Sensitization of Austenitic Stainless Steel I. Controlled Purity Alloys," Journal Corrosion, Vol. 38, No. 9, p 468, 1982.

VITA

The author was born October 24, 1957 in Las Tabls, Republic of Panama.

He attended the Instituto Politecnico Nacional, Mexico D.F. from January 1977 to 1981 were he received his B.S. in Metallurgical Engineering.

He was a part time instructor at Universidad Technologica de Panama from April 1982 to 1984 and full time instructor from April 1985 until the Fall of 1986.